Infocommunications Journal

A PUBLICATION OF THE SCIENTIFIC ASSOCIATION FOR INFOCOMMUNICATIONS (HTE)

SEPTEMBER 2017 Volume IX Number 3 ISSN 2061-2079

Technically Co-Sponsored by

IEEE ComSoc™ IEEE Communications Society

hte

IEEE HUNGARY SECTION

Indexing information

Infocommunications Journal is covered by Inspec, Compendex and Scopus.
Infocommunications Journal is also included in the Thomson Reuters – Web of ScienceTM Core Collection, Emerging Sources Citation Index (ESCI)

Infocommunications Journal

Technically co-sponsored by IEEE Communications Society and IEEE Hungary Section

Supporters

FERENC VÁGUJHELYI – president, National Council for Telecommunications and Information Technology (NHIT)
GÁBOR MAGYAR – president, Scientic Association for Infocommunications (HTE)

Editorial Office (Subscription and Advertisements)**:**
Scientic Association for Infocommunications
H-1051 Budapest, Bajcsy-Zsilinszky str. 12, Room: 502
Phone: +36 1 353 1027
E-mail: info@hte.hu • Web: www.hte.hu

Articles can be sent also to the following address:
Budapest University of Technology and Economics
Department of Telecommunications and Media Informatics
Tel.: +36 1 463 1102, Fax: +36 1 463 1763
E-mail: vida@tmit.bme.hu

Subscription rates for foreign subscribers: 4 issues 10.000 HUF + postage

Publisher: PÉTER NAGY

HU ISSN 2061-2079 • Layout: PLAZMA DS • Printed by: FOM Media

A Little Less Interaction, A Little More Action: A Modular Framework for Network Troubleshooting

István Pelle, Felicián Németh and András Gulyás

***Abstract*—Requirements of an ideal network troubleshooting system dictate that it should monitor the whole network at once, feed results to a knowledge-based decision making system and suggest actions to operators or correct the failure, all these automatically. Reality is quite the contrary, though: operators separated in their cubicles try to track down complex networking failures in their own way, which is generally a long sequence of manually edited parallel shell commands calling rudimentary tools. This process requires operators to be "masters of complexity" (which they often are) and continuous interaction. In this paper we aim at narrowing this huge gap between vision and reality by introducing a modular framework capable of *(i)* formalizing troubleshooting processes as the concatenation of executable functions [called troubleshooting graphs (TSGs)], *(ii)* executing these graphs via an interpreter, *(iii)* evaluating and navigating between the outputs of the functions and *(iv)* sharing troubleshooting know-hows in a formalized manner.**

***Index Terms*—Computer networks, troubleshooting, decision support.**

I. Introduction

TROUBLESHOOTING a communication network was never an easy problem. Finding causes of errors and failures, tracking down misconfigurations in the increasingly complex interconnection networks of heterogeneous networking devices is quite a challenge. What is more, the prevalence of increasingly complex software components, due to the upcoming software defined networks (SDNs), adds distributed software debugging as an additional issue to deal with. To cope with this increasing complexity, the networking research community suggests the use of knowledge-based decision support together with the standard network monitoring and diagnostic tools, and the conversion of troubleshooting into a highly automated process. Reality seems to reside very far away from this vision. Real operators tend to use the most basic diagnostic tools for monitoring the network, and rely on their own brilliance and programming skills when digging out the root causes of errors in an ad-hoc manner from the reports of these tools. Even if this approach works well in practice, it requires extremely skilled operators who can keep in mind all the details of the network under scrutiny and their continuous interaction usually is wasted on rummaging in the logs of the tools used by them.

As we see, the reason for this huge gap between the ideas and reality is threefold. First, there is no usable, implementation oriented formal description of the troubleshooting processes. Second, there is no platform capable of executing formally defined troubleshooting processes while giving prompt and systematic access to the outputs of the used tools. Finally, there is no existing platform that could integrate existing troubleshooting tools and decision support methodologies in a flexible manner. In lack of formalism and integrated execution platform, operators cannot share and re-use each other's troubleshooting know-hows in a structured way, thus knowledge is not accumulated but remains sporadic as operators treat every specific failure in their own ad-hoc way.

Based on these observations, our contribution will be threefold. First, we propose a formalization of troubleshooting processes in the form of troubleshooting graphs (TSGs)—complete with a description language to define them—, which let operators specify the steps of tracking down network failures in a structural manner. Once created, TSGs can make their solutions ready-to-share and re-usable. Second, we propose a modular execution framework capable of running TSGs and offering on demand fast semantic navigation among the outputs of the tools used in the troubleshooting process. Finally, we present a complete prototype system capable of defining, executing and analyzing TSGs.

The rest of our paper is structured as follows: in Section II we give a brief overview on the related work in both literature and practice. Section III lists the principles of our proposed modular troubleshooting framework, followed by the illustration of its operation over an SDN example in Section IV and an example for traditional networks in Section V. Section VI presents the fundamentals of our prototype, *Epoxide*, which is complemented with a complex illustrative case study in Section VII. Finally, we conclude the paper and give directions for future works in Section VIII.

II. State of the Art in Network Troubleshooting

From the great volume of related literature we highlight here the two main constituents of troubleshooting systems. The first is clearly the area of *network monitoring and diagnostic*

I. Pelle and F. Németh are with Budapest University of Technology and Economics, Hungary, with HSNLab, Dept. of Telecommunications and Media Informatics. e-mail: {pelle, nemethf}@tmit.bme.hu

A. Gulyás is with Budapest University of Technology and Economics, Hungary, with HSNLab, Dept. of Telecommunications and Media Informatics and with MTA-BME Information Systems Research Group and was supported by the János Bolyai Fellowship of the Hungarian Academy of Sciences. e-mail: gulyas@tmit.bme.hu

The research leading to these results was partly supported by Ericsson and has received funding from the European Union Seventh Framework Programme under grant agreement № 619609.

tools, of which main purpose is to seek for symptoms of specific failures. The palette is very broad here, ranging from the most basic tools (like ping, traceroute, tcpdump, netstat, nmap [1] or GNU Debugger (GDB)), through monitoring protocols (such as SNMP and RMON [1]), configuration analyzers (e.g. Splat [2]), performance measurement tools (e.g. iperf [1]) and packet analyzers (like Wireshark), to the more complex ones, such as NetFlow, HSA [3], [4] and ATPG [5]. On top of these, SDN specific tools have added a whole new segment targeting the investigation of specific parts of the architecture. Tools such as Anteater [6], OFRewind [7], NetSight [8], VeriFlow [9], NICE [10], SOFT [11], FORTNOX [12] and OFTEN [13] all fill a niche in SDN troubleshooting.

One level up, the output symptoms of these tools can be aggregated and fed into different *automatic reasoning solutions*. The first representatives of these were created as early as the second half of the 1980s [14] targeting the discovery of failures in telecommunication networks. Early on, rule-based methods were used to resolve issues by using *if–then* statements [15]. Later case-based reasoning [16] and model-based [17] methods were developed. The former utilized a collection of previous cases as a basis for failure analysis, while the latter used models of structural and functional behavior to reason about network issues. Fault-symptom graphs [18] and dependency or causality graphs [19], [20] introduced the concept of tracking failures using graphs that created connections between symptoms, detection and root causes. This concept led to the application of Bayesian networks [21], [22] where belief—in the most probable failure root cause—propagation is based on a probabilistic model.

A. What We See in Current Practice

Despite the readily available set of advanced troubleshooting tools and decision support mechanisms, operators seem to use the most rudimentary tools (like ping, traceroute, tcpdump etc.) while they completely rely on their minds as a knowledge-base. For testing this, we conducted an in-house survey querying which type of problems local administrators run into most frequently and what network troubleshooting tools they use most commonly. The results, we found were completely in accordance with those outlined in [23]. Most problems were caused by connectivity issues that arose from a variety of reasons ranging from hardware failures to configuration changes that became necessary due to security issues. Used troubleshooting tools show similarities also: mostly simple task specific tools are utilized, in certain cases combining them in a script to explore typical failures. Network information is usually stored in simple spreadsheets and proprietary monitoring or troubleshooting tools are used only when they have a low cost—or are preferably free. We found that automatic tools are less frequently used and manual troubleshooting dominates problem solving.

To get a deeper sense of the process, imagine the following scenario: an operator wants to monitor certain traffic flows in an SDN network and analyze whether these flows comply with certain criteria. By applying manual troubleshooting using multiple shells, our fictional operator has to connect to different devices—SDN switches and hosts—run software tools to extract traffic data and then filter these to obtain the flows. This process relies on the application of repetitive tasks—login and invocation of specific tools—and analyzing textual data. This process poses four main problems. *(i)* When historical data is needed, the tools cannot be closed, thus they quickly overpopulate the working environment. *(ii)* While the process is extremely flexible—as operators use tools of their choosing in the way and logic they see fit—, processing the data quickly becomes overwhelming and inefficient without computerized help. *(iii)* There is no clear way that the process—the steps to be taken—can be recorded and later reused in a flexible enough manner. *(iv)* The process is unorganized, thus operators' time is spent mostly on filtering and finding the correlation between the different outputs and keeping in mind the mapping between different shells and devices.

III. Design Principles of a Modular Framework for Network Troubleshooting

Instead of proposing a new troubleshooting tool or another decision support mechanism, we suggest here a framework[1] capable of *combining* existing (and future) special-purpose tools and reasoning methodologies in a modular fashion. Our concept builds on the observation that operators combine different troubleshooting tools to find out the root cause of a network issue. In the following sections, we go through the main notions that we use to describe such troubleshooting processes and the fundamentals of our framework capable of executing troubleshooting graphs (TSGs).

A. Nodes: Wrappers Around Troubleshooting Tools

First we define an abstraction that incorporates the basic elements of a troubleshooting process: *nodes* are wrappers around troubleshooting tools or smaller, processing functions. These are considered as black boxes hiding their internal operation from the outside (see Fig. 1). Operators have three types of interfaces for communicating with nodes. On *inputs* they execute operations (e.g. a text stream to process or clock ticks). *Configuration arguments* relay static parameters. Finally, *outputs* relay the exact output of the wrapped tool or provide extra processing before generating results.

Three stages make up the life cycle of a node. Nodes enter their *initialization* stage only once, where environment setup is performed, including resource allocation and initial configuration. At the execution stage, nodes read the data arriving on their inputs and query the wrapped process or function. Analysis or modification on the wrapped tool's output is also performed here. The node is constantly in this stage when it has been initialized but not yet been terminated. Finally, the node reaches the termination stage when it is being stopped. This stage is responsible for clearing up allocated resources and terminating wrapped processes.

[1]Our initial research and implementation of a subset of current framework functionality is discussed in [24].

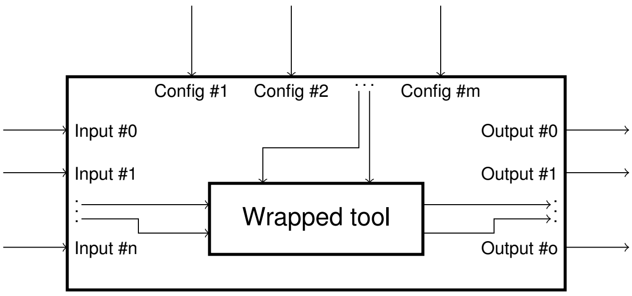

Fig. 1: A conceptual node.

B. Edges: Accessible Data Transfer

We use *edges* to describe the connections between nodes. Besides specifying the nodes to connect, the main feature required from edges is to provide accessibility for node outputs: information over the edges is observable and modifiable on demand by operators. When access is given to edges, operators can analyze troubleshooting processes on the lowest levels. By making historical data available on edges, backtracking network condition changes becomes feasible during runtime. Modifiable edges provide the additional benefit of direct operator interaction with nodes, which is helpful for instant testing purposes. This method also helps channeling—otherwise unobtainable—data into our system from the network environment.

C. The Troubleshooting Graph

By leveraging the power of wrapper nodes and accessible edges, troubleshooting processes can be formalized as TSGs: series of tools and transformations.

Besides the simple concatenation of nodes, creating branches is possible through special purpose *decision* nodes. These nodes are processing nodes capable of analyzing incoming data and matching them against a specific criteria set. Such nodes can provide generalized decision making apparatus that can combine results arriving from different nodes and implement arbitrary decision functions to analyze and evaluate them.

For a text-based representation of TSGs, we define a simple Click-inspired [25] description language. Such language fits perfectly to our concept as we look at nodes as black boxes that have inputs, outputs and configuration arguments, which the language supports by default. Port-based explicit node linking is also a feature that we make good use of. An exemplary TSG and its definition using the language is given in Section IV.

D. Execution Framework for TSGs

In order to bring the TSG concept closer to implementation, we designed our execution framework around three cornerstones. *(i) Interpretation*: since a TSG is only a formal description, the framework provides a parser to interpret the graph. *(ii) Execution*: the TSG concept describes how to connect tools to each other but it does not deal with the problem of when and how a node's life cycle is managed and how a node is notified when its inputs are updated. *(iii) Navigation options*: the benefit of handling interconnected troubleshooting tools as a graph is that it creates a natural order in the troubleshooting process. In order to better manage the complex information set contained in the graph, the framework provides different apparatuses to aid observing the execution state and navigating through the graph.

E. Recommendation System and Knowledge Sharing

The framework provides a recommendation system that is able to suggest new nodes for operators, based on their current setup, by searching for similarities in a TSG repository. Operators can upload their existing TSGs to this repository hereby promoting knowledge sharing.

IV. AN SDN EXAMPLE USING TSGS

In order to solve our running example from Section II-A, instead of manually gathering information about the flows, operators can create a TSG—such as the one shown in Fig. 2—that automates the process for them.[2] They can leverage a unified interface for accessing different OpenFlow capable entities by using nodes to interact with different controller platforms and Open vSwitch (OVS) switches. These nodes are able to collect dapatapath identifiers (DPIDs) and flow statistics information. Additionally, we created processing nodes for filtering flow statistics on a flow space[3] basis.

In line 1 of the example of Fig. 2, we define nodes querying DPIDs from the controller[4] on a timely basis by writing expressions that are always terminated by semicolons. Nodes can be defined by assigning an instance name to a wrapper node using the `::` operator and linked with edges to other nodes using the `->` linking operator. For simplicity, the instance name can be omitted if the node is not referenced in the code later on (see the `Dpids` node). Configuration arguments follow the node instance assignment in parentheses. Let's stop now to have a closer look at the `Dpids` node. On its single output, the node relays the DPIDs of the switches connected to a certain SDN controller, each time it receives an enabling signal on its single input. The single configuration argument specifies the location of this controller. In the initialization stage, the node sets up connection to the controller. At execution time, it accesses the controller's specific API to query the DPID information, while at the termination stage, the ongoing processes are stopped and the connection to the controller is closed.

Linking operators always have the list of node outputs on their left side and the list of inputs on their right side—as in line 7 of the example. Multiple edges can also be created between two nodes in a single expression this way. Outputs and inputs are always referred to with their zero-based indices. In case only the 0^{th} input or output appears in a linking expression, one can omit its index, as depicted in line 1. In

[2]With an appropriate node repository, only the connections need to be correctly specified among nodes.

[3]Those flow table entries make up a flow space that match given source and destination point pairs.

[4]Nodes accessing POX, Floodlight and OpenDaylight controllers are currently available.

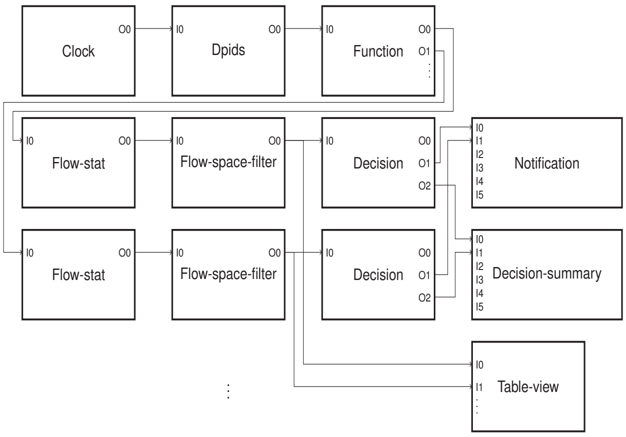


```
Clock(1) -> Dpids(<controller location>)
-> f :: Function(...)
-> Flow-stat(...)
-> filter1 :: Flow-space-filter(...)
-> d1 :: Decision(...)[1]
-> n :: Notification(...);
d1[2] -> [0]summary :: Decision-summary();
filter1 -> table :: Table-view()
--> view :: View();
f[1] -> Flow-stat(...)
-> filter2 :: Flow-space-filter(...)
-> d2 :: Decision(...)[1] -> [1]n;
d2[2] -> [1]summary --> [1]view;
filter2 -> [1]table;
...
```

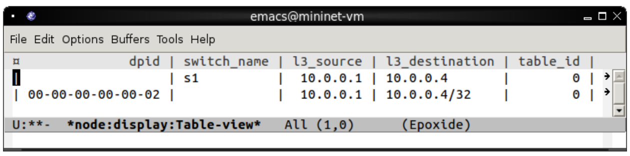

Fig. 2: An SDN example: graphical representation of a TSG querying flow statistics (top), its formal definition (middle) and the output of the Table-view node displaying the results (bottom). For brevity, the formal definition is shortened.

Listing 1: Formal description of the TSG.

```
1  ping :: Ping(localhost, <address of the server>);
2  ifconfig :: Ifconfig(localhost);
3  arp :: Arp(localhost, nil, -n);
4  ping-decision :: Decision(...);
5  ifc-decision :: Decision(...);
6  arp-decision :: Decision(...);
7  ping -> ping-decision;
8  ifconfig -> ifc-decision;
9  arp -> arp-decision;
10 ping-decision[1] -> ifconfig;
11 ifc-decision -> Function(ifconfig-get-interfaces,
12                          'input-0)[0, 0]
13 -> [0, -2]arp;
14 ping-decision[2] -> ds :: Decision-summary();
15 ifc-decision[2] -> [1]ds;
16 arp-decision[2] -> [2]ds;
```

our language—unlike in Click—one can connect outputs to configuration arguments as well, which enables the flexible dynamic configuration of nodes. This uses the same syntax as the output–input linking.

After querying the list of DPIDs, the Function node—that can wrap any preexisting function—splits it and passes the data to further nodes that query flow statistics—by wrapping the ovs-ofctl tool—from their assigned switches. With the addition of flow space filtering nodes, the operator can select only the flows under scrutiny and display the results in a table format, as depicted by the bottom part of Fig. 2. By appending Decision nodes to the filtering nodes, the operator can make an automatic comparison of the current state of the switches to a predefined criteria set—that might come from a formal definition of the network policy or the controller itself. This could reveal synchronization issues between the devices or misdirection of the traffic caused by a software failure. The results are then displayed in a table format using a Decision-summary node—that interprets decisions by signaling "error" codes with visual aids—and a Notification node that provides desktop notifications whenever a test fails. By connecting Gdb nodes—wrapping the GNU Debugger—with the Decision nodes, the operator could remotely connect to software switches or to the controller for an in-depth analysis of the problem.[5] (Decision nodes are only briefly discussed here, see Section VI-B for more details.)

V. An Example for Traditional Networks

In order to locate errors in a traditional network, a set of currently used free tools can be applied. In a scenario where we want to detect different errors, we can chain these tools together, using TSGs, in such a way that Listing 1 shows. For brevity, we show only the instructions used for creating a TSG that performs a connection test and if that is unsuccessful, checks the local machine's network configuration. This exemplary TSG is not complete (e.g. routes and firewall rules are not checked[6]). We use extended wrapper nodes for the tools, so—on top of their basic functionality—we assume that Host, Ifconfig and Arp nodes provide means to exclude specified interfaces from their outputs, the Traceroute node is able to relay the last hop until which the traffic is traceable and the Route and Iptables nodes are capable of displaying only those rules that apply to certain IP addresses[7]. Decision nodes in the TSG evaluate the correctness of given inputs, while the Decision-summary node creates a human readable interface for them.

In order to perform a connection test between the current host and a server, we use a wrapper node for the ping tool in line 1. Lines 2–3 create tests for checking the local host's configuration using the ifconfig and arp tools. In order to automatically evaluate these, we defined three Decision

[5] A live action demo on a similar, albeit simpler, case can be watched at [26]: https://www.youtube.com/watch?v=HsiGFR0QirE

[6] Instructions for creating nodes for those tests, however, would be written using the same philosophy shown here.

[7] These assumptions are not unrealistic since wrapper nodes can extend the wrapped tool's functionality in such convenient ways.

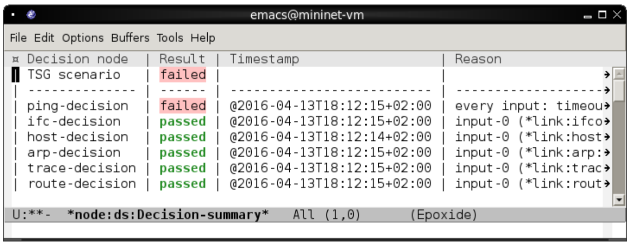

Fig. 3: Summarizing a troubleshooting scenario.

nodes. `ping-decision` checks whether the `ping` was successful. `ifc-decision` uses a custom function to validate the interface configuration returned by the `ifconfig` node. The `arp-decision` node performs a simple check to test whether there are entries in the Address Resolution Protocol (ARP) cache. These Decision nodes are then connected with their respective wrapper nodes in lines 7–9. In order to check the local host's configuration only when the connection test was unsuccessful, we need to connect the `ifconfig` node to the negative output of the `ping-decision` node—line 10 implements that. If there are interfaces on the host that are correctly configured, we need to check whether the host can register the layer 2 addresses from its network. We defined a `Function` node in line 11 in order to retrieve the interface names from the output of the `ifc-decision` and fed these to the `Arp` node. Finally, we defined a `Decision-summary` node in lines 14–16 to display information collected from every Decision node in a summarizing table.

We executed the extended version of this TSG in a home networking environment, where a Linux host was connected to the residential gateway via WiFi connection. A possible output of the `Decision-summary` node is shown in Fig. 3. The node gives the results of the individual decisions in the TSG as well as an overall evaluation of the current troubleshooting scenario: connection with the remote server cannot be established but the configuration of the current host seems to be fine. The most basic assumption at this point can be that the problem is caused by either the residential gateway or it is located at the Internet Service Provider's side.

These simple examples attest that by using TSGs, we can achieve a state of automation where operators can recognize failure modes at a glance by looking at the error codes, or can further delve into details by navigating through the outputs of nodes. Using the navigation options provided by the framework, the operator can walk through the troubleshooting process in an orderly fashion. Results are going to be displayed according to the workflow, laid out when setting up the process of locating the issue.

By offering proper formalization, TSGs—or their subgraphs—can be reused in similar scenarios with slight adjustments to the node configuration arguments. Besides re-usability, TSGs can act as a technique to collect troubleshooting know-hows. Once a network problem is uncovered using a TSG, it automatically becomes a guideline for discovering future similar issues. By collecting a library of these, operators can greatly decrease problem solution times and the efficiency of knowledge transfer to new operators can also increase. If TSGs are not only collected within a closed environment—i.e. within a company—but are shared with a greater audience, they can prove to be beneficial for the whole networking community. If a wide TSG library is paired with problem descriptions and solutions, new nodes and test cases can be recommended to an operator, based on previous cases described by TSGs in the library.

VI. PROTOTYPE

For proofing the concept of our framework, we created a prototype implementation, named Epoxide, using GNU Emacs as a platform. Emacs is an extensible, customizable text editor, its central concept, the buffer, is responsible for holding file contents, subprocess outputs, providing configuration interfaces, etc. By its extensible nature, Emacs offered a particularly good platform to build Epoxide upon. Emacs supports, via its advanced text manipulation and documentation functions, writing TSG definitions that we store in `.tsg` configuration files. We implemented our execution framework and wrapper nodes using Emacs's own Lisp dialect, Emacs Lisp. Nodes and their outputs are assigned to Emacs buffers for observability. Node interface and connection information is stored in buffer local variables. We note that while Emacs proved to be a good fit for our notions, the concept described in Section III can be implemented on other platforms as well.

A. Framework Functions

Epoxide provides two methods to create TSGs. The first option is building the graph by interpreting its definition written in our description language. Opening a `.tsg` file in Emacs automatically loads Epoxide and interprets the TSG stored in it. Using this method, graphs can be saved and later reused and shared. Since we added self-documenting capabilities to nodes and leveraged functionality provided by Emacs's *ElDoc* package, the framework offers hints on node interfaces during TSG definition. Syntax highlighting helps to differentiate semantic units at this stage and when Emacs's *Auto Complete* package is installed, it can provide intelligent code completion for setting up nodes. At first, the parser collects the nodes, their configuration arguments and the links between the nodes. The framework assigns unique names to node objects and outputs and maps these to buffers where nodes can write directly during their execution stage. This method can also be used to modify TSGs by way of editing the `.tsg` file and reevaluating it. A downside is that buffer contents prior to the modification get lost.

As a second option, we provide a method for incrementally building TSGs at run time using a drag and drop method. This method has the benefit that operators can monitor the output of the used tools and adjust their methodology to the results they have acquired until that point (which is fully in line with current practice). The parser creates the objects for the nodes and interconnections, and commits these to the `.tsg` file. Run-time modification of the graph—node reconfiguration and relinking—is provided by this functionality as well via an Emacs widget based interface. These two methods can be used

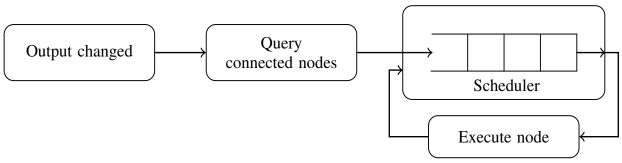

Fig. 4: Scheduling of node execution.

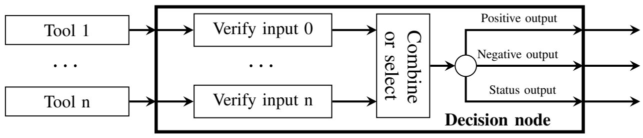

Fig. 5: Schematics of a Decision node.

in conjunction and offer flexibility while retaining the benefit of being able to store troubleshooting scenarios.

Once TSG execution is started, the framework takes care of node events, as depicted in Fig. 4. A scheduler is created—using the *timerfunctions* package—that handles a queue for registering node output changes. Each time an output has changed, the framework queries which nodes have that as their input. These destination nodes are then inserted to the end of the queue. Parallel to this, a simple scheduling mechanism is running that always takes the first item from the beginning of the queue and sends a signal to that node to enter into the execution stage. When the call returns, the scheduler moves to the next node in line and so on.

Basic navigability among the created buffers is provided by Emacs key bindings. Epoxide supplies the apparatus to move from one node buffer to its output buffers or to the next node's buffer (in forward or backward direction). To traverse a TSG, a visualization can be used also, supported by the Emacs *COGRE* package. When the *Graphviz* external software is installed, the displayed graph can be drawn using an automatic layout for better visual clarity. Semantic grouping of the created buffers is provided using the *Ibuffer* package: a dynamic list is displayed that aggregates buffers based on their types and roles in the current context. Custom grouping of buffers is also available via a special node class, a `View`, that can collect nodes or their outputs and display them together.

The current implementation of Epoxide provides a module for collecting TSG related data and supplying node recommendations. We created the instrumentation for basic case-based reasoning where currently available TSGs are considered as descriptions of previous troubleshooting cases. These TSGs are indexed and their data—together with information from the current TSG—is passed to a recommender. The recommender then can suggest nodes based on these pieces of data. We created an interface in the framework to which recommenders, developed by third parties, can connect as well. By now, we have implemented the most basic recommender that suggests the most popular nodes and displays them using Emacs's *Ido* package. Most popular nodes are computed by counting every node in all previously written TSGs and ordering them in the descending order of their cumulative count. Nodes that are already used in the current TSG, are excluded from the suggestion list.

B. Branching Nodes

When creating the apparatus that enables conditional branching in Epoxide, the most basic expectation was to *(i)* provide functionality to analyze and evaluate the output of any node and, based on the result, *(ii)* create branches in a TSG, the same way a decision would in a flow chart. Additionally, we wanted to have the ability to *(iii)* select among different inputs or to use a combination of them. This criterion was inspired by how nodes work in a Bayesian network: they receive the results of lower level nodes and calculate their outputs based on that. To satisfy these criteria, we implemented a single *Decision node*. Since nodes can be added to Epoxide in a modular fashion, this is only one possible implementation that satisfies our initial criteria. Operators are free to add their own version. A *Decision-summary node* was developed in conjunction, for summarizing the outputs of such nodes.

Fig. 5 shows the schematics of our Decision node. The node can attach to any wrapper node[8] and incoming data is first verified (as per *(i)*): compliance with a certain criteria set is determined. The node can use any function for verification that has at least one argument (the input) and can return false, when verification failed, or any string otherwise. When verification of the inputs is finished, further processing can be done using a second stage function, in accordance with *(iii)*. An operator can use a function to select an input with, for example, the *or* function: the first of the inputs that passed verification is going to be the result of this stage. Other functions can implement more complex processing, like in the aforementioned Bayesian network example where the result would be a probability value. Such second stage functions should return a string in case of a positive decision or false otherwise. We defined two node outputs to relay these return values (as per *(ii)*). The first displays information in the positive case, the second in the negative. We implemented an additional output for interoperating with Decision-summary nodes.

C. Implementing Nodes

The modular architecture of Epoxide makes it possible for anyone to implement new nodes. A node developer—who implements a node—has to create separate node definition files that contain Emacs Lisp code to provide self-documentation for nodes and implement the three life cycle stages via functions. For proper interaction with nodes, the node definition files and these functions should comply with a fixed naming scheme. Node self-documentation functions should provide information about node interfaces and could also implement validation functions to check the compliance of arguments with certain criteria. The functions implementing the separate node life cycle stages are called by the framework on specific occasions. The initialization function is evoked after the buffers belonging to the node are set up. The execution

[8]The node is also prepared to handle the asynchronism and the different output formats of the wrapper nodes.

function is called every time a change occurs on any of the node's inputs. Finally, the termination function is invoked before the framework closes the buffers associated with the node. These functions can draw on common node functions provided by the framework. Epoxide implements functions for setting up node buffers with basic data, reading inputs and configuration arguments, writing outputs and handling remote access using Emacs's *Transparent Remote Access, Multiple Protocols (TRAMP)* package.

VII. A Case Study: Troubleshooting in Service Function Chaining

One of the main goals of the UNIFY project[9] was to design a Service Function Chaining control plane architecture and implement a proof-of-concept prototype. Additionally, the project also introduces the concept of Service-Provider DevOps to combine the developer and operational workflows in carrier grade environments. DevOps results in faster deployment cycle of novel networking services. Instead of designing complex services as a whole, these services are assembled from atomic *network functions*. However, fast deployment cycles require faster testing phases and troubleshooting in the operational environment. Even when a new service is created by re-using components of previous ones, it is still going to be different enough from earlier scenarios to implicate new troubleshooting challenges. In these cases, previous knowledge is not always directly applicable. By providing an integrated platform for running troubleshooting tools and an apparatus to automatize their execution, our tool makes the formation of new troubleshooting scenarios easier, thus enabling quicker service deployment.

Epoxide has a central role in the multipurpose demonstrator showcasing major results of the project [27]. Using its dedicated and general purpose wrapper nodes, it orchestrates multiple components in a semi-automatic troubleshooting scenario. Epoxide needs to reveal a configuration error resulting in erroneous imbalance of the traffic loads of OpenFlow switches instantiated as network functions. The novel components, which Epoxide interacts with, include a flexible messaging bus (Double Decker), a tool that calculates aggregated performance metrics derived from data queried from hierarchical time series databases [Recursive Query Engine (RQE)], and a test packet generator for pinpointing errors in OpenFlow switches (AutoTPG).[10] The use of Epoxide significantly shortens the time spent on analyzing network state, compared to a manual troubleshooting scenario.

Fig. 6 highlights the main system components and the sequence of interactions. First, a monitoring component detects the resource imbalance (this takes a couple of seconds) that automatically triggers the execution of the troubleshooting process in Epoxide which executes a TSG tailored for this scenario (step 1). In step 2, Epoxide asks the Recursive Query Engine to verify the prevalence of the error. After querying historical measurement data—that takes 1-2 seconds in

[9]https://www.fp7-unify.eu

[10]Detailed description of these tools and the demonstrator can be found in [27].

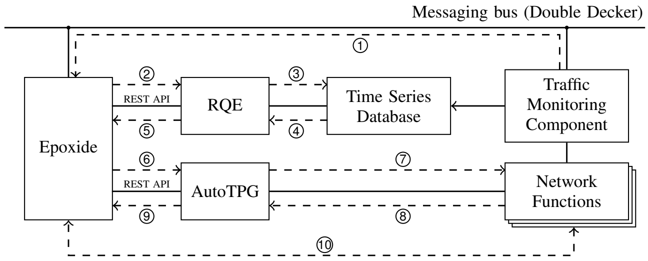

Fig. 6: Simplified view of the UNIFY demo architecture and sequence of interactions.

steps 3–4—RQE notifies Epoxide at step 5. In step 6, Epoxide starts and configures AutoTPG and asks it to test switches one by one. AutoTPG tests the correctness of the switches in steps 7–8 (this test runs in the order of minutes) and returns the result to Epoxide in step 9. Finally, Epoxide queries the flow-entries of the erroneous switch (step 10), and presents those in tabular form to the user to help further investigating the problem manually. Since Epoxide is responsible for calling other tools and performing simple analysis on their outputs, it adds very little reaction time overhead. The complete runtime of the scenario mostly comprises of the runtime of the used tools, mainly that of the AutoTPG.

The demo TSG contains a wrapper node for the messaging bus, but communicates with the other tools via `Rest-api` nodes that use JSON-formatted inputs and emit JSON-formatted outputs. We introduced formatting and JSON filtering nodes in order to assemble and parse these JSON requests and responses. Another general purpose node was also developed that is able to call any command line tool. We had good use of this node when running *ssh* commands to query and modify the configuration of a remote network function.

Epoxide exhibits properties that make it an ideal testing and troubleshooting tool for Service Function Chaining. First, the TSG language is an enabler of fast hypotheses testing and small feedback cycles because it allows connecting existing special purpose troubleshooting tools at an abstract level. Second, the test generation process can be further shortened by simply re-using parts of existing `.tsg` definitions. Finally, complex decision logics can be based on service-specific monitoring and troubleshooting tools by writing simple wrapper nodes around these tools.

VIII. Conclusion and Future Work

While our modular framework proposed here is capable of flexibly combining various troubleshooting tools for tracking down networking issues, and the TSG concept enables the accumulation and sharing of troubleshooting related knowledge, the current prototype implementation should be extended in many aspects. Of course, a large library of wrapper nodes should be added to incorporate more and more troubleshooting tools. Besides this natural option, we outline here some future directions, the framework could benefit from.

Although present implementation supports the addition of new node recommenders, the currently implemented one provides only a basic functionality. We consider this a basis to implement better recommenders. Suggestions could be made more relevant by taking the environment of the nodes into consideration and suggesting node configurations as well. The process could further be supported by using a community-based repository of TSGs where TSGs can be analyzed and used for supplying better suggestions.

With the help of an appropriate failure propagation model and formal description of the network policy, we believe, TSGs containing network tests and basic evaluations can be generated with little operator intervention or totally unsupervised. By adding the possibility to create hierarchical TSGs, Epoxide could create more complex tests that are selected and configured automatically depending on results acquired from the network at real time.

REFERENCES

[1] Sloan, J. D., *Network Troubleshooting Tools*. O'Reilly, 8 2001.

[2] Abrahamson, C., Blodgett, M., Kunen, A., Mueller, N., and Parter, D., "Splat: A Network Switch/Port Configuration Management Tool," in *Proceedings of the 17th Conference on Systems Administration (LISA 2003)*, 2003.

[3] Kazemian, P., Chan, M., Zeng, H., Varghese, G., McKeown, N., and Whyte, S., "Real Time Network Policy Checking Using Header Space Analysis," in *NSDI*, 2013, pp. 99–111.

[4] Kazemian, P., Varghese, G., and McKeown, N., "Header Space Analysis: Static Checking for Networks," in *NSDI*, 2012, pp. 113–126.

[5] Zeng, H., Kazemian, P., Varghese, G., and McKeown, N., "Automatic test packet generation," in *Proceedings of the 8th international conference on Emerging networking experiments and technologies*. ACM, 2012, pp. 241–252.

[6] Mai, H., Khurshid, A., Agarwal, R., Caesar, M., Godfrey, P. B., and King, S. T., "Debugging the Data Plane with Anteater," in *Proceedings of the ACM SIGCOMM 2011 Conference*, ser. SIGCOMM '11. New York, NY, USA: ACM, 2011, pp. 290–301. [Online]. Available: http://doi.acm.org/10.1145/2018436.2018470

[7] Wundsam, A., Levin, D., Seetharaman, S., Feldmann, A. *et al.*, "OFRewind: Enabling Record and Replay Troubleshooting for Networks," in *USENIX Annual Technical Conference*, 2011.

[8] Handigol, N., Heller, B., Jeyakumar, V., Mazieres, D., and McKeown, N., "I know what your packet did last hop: Using packet histories to troubleshoot networks," in *Proc. USENIX NSDI*, 2014.

[9] Khurshid, A., Zhou, W., Caesar, M., and Godfrey, P., "Veriflow: verifying network-wide invariants in real time," *ACM SIGCOMM Computer Communication Review*, vol. 42, no. 4, pp. 467–472, 2012.

[10] Canini, M., Venzano, D., Peresini, P., Kostic, D., Rexford, J. *et al.*, "A NICE Way to Test OpenFlow Applications," in *NSDI*, vol. 12, 2012, pp. 127–140.

[11] Kuzniar, M., Peresini, P., Canini, M., Venzano, D., and Kostic, D., "A soft way for openflow switch interoperability testing," in *Proceedings of the 8th international conference on Emerging networking experiments and technologies*. ACM, 2012, pp. 265–276.

[12] Porras, P., Shin, S., Yegneswaran, V., Fong, M., Tyson, M., and Gu, G., "A security enforcement kernel for openflow networks," in *Proceedings of the first workshop on Hot topics in software defined networks*. ACM, 2012, pp. 121–126.

[13] Kuzniar, M., Canini, M., and Kostic, D., "OFTEN testing OpenFlow networks," in *Software Defined Networking (EWSDN), 2012 European Workshop on*. IEEE, 2012, pp. 54–60.

[14] Mathonet, R., Van Cotthem, H., and Vanryckeghem, L., "DANTES An Expert System for Real-Time Network Troubleshooting," in *Proceedings of the 10th International Joint Conference on Artificial Intelligence*, 1987, pp. 527–530.

[15] Hitson, B. L., "Knowledge-Based Monitoring and Control: An Approach to Understanding the Behavior TCP/IP Network Protocols," in *Symposium proceedings on Communications architectures and protocols*, vol. 18, 1988.

[16] Lewis, L., "A Case-Based Reasoning Approach to the Management of Faults in Communications Networks," in *Twelfth Annual Joint Conference of the IEEE Computer and Communications Societies*, 1993.

[17] Jakobson, G. and Weissman, M., "Real-time telecommunication network management: extending event correlation with temporal constraints," in *Proceedings of the fourth international symposium on Integrated network management IV*, 1995, pp. 290–301.

[18] Reali, G. and Monacelli, L., "Definition and performance evaluation of a fault localization technique for an NGN IMS network," in *IEEE Transactions on Network and Service Management*, 2009, p. 6(2):122136.

[19] Lu, J., Dousson, C., Radier, B., and Krief, F., "Towards an Autonomic Network Architecture for Self-healing in Telecommunications Networks," in *Mechanisms for Autonomous Management of Networks and Services*, vol. 6155, 2010, pp. 110–113.

[20] ——, "A Self-diagnosis Algorithm Based on Causal Graphs," in *The Seventh International Conference on Autonomic and Autonomous Systems*, 2011.

[21] Charniak, E., "Bayesian networks without tears: making Bayesian networks more accessible to the probabilistically unsophisticated," in *AI Magazine*, vol. 12, 1991, pp. 50–63.

[22] Khanafer, R., "Automated diagnosis for UMTS networks using Bayesian network approach," in *IEEE Transactions on Vehicular Technology*, 2008, p. 57:24512461.

[23] Zeng, H., Kazemian, P., Varghese, G., and McKeown, N., "A Survey on Network Troubleshooting," 2014.

[24] Pelle, I., Lévai, T., Németh, F., and Gulyás, A., "One tool to rule them all: A modular troubleshooting framework for SDN (and other) networks," in *Proceedings of the 1st ACM SIGCOMM Symposium on Software Defined Networking Research*, 2015.

[25] Kohler, E., Morris, R., Chen, B., Jannotti, J., and Kaashoek, M. F., "The Click modular router," *ACM Transactions on Computer Systems (TOCS)*, vol. 18, no. 3, pp. 263–297, 2000.

[26] Lévai, T., Pelle, I., Németh, F., and Gulyás, A., "Epoxide: A modular prototype for sdn troubleshooting," in *Proceedings of the 2015 ACM Conference on Special Interest Group on Data Communication*, 2015, pp. 359–360.

[27] Marchetto, G. and Sisto, R. (editors), "Deliverable D4.3: Updated concept and evaluation results for SP-DevOps," in *eprint arXiv:1610.02387*, 2016.

István Pelle received M.Sc. degree in Computer Engineering at Budapest University of Technology and Economics, Budapest, Hungary in 2015. Currently he is pursuing the Ph.D. degree with Budapest University of Technology and Economics. His research interests include software defined networks and network troubleshooting.

Felicián Németh received his M.Sc. degree in Computer Science from BME in 2000. He is a research fellow at the Department of Telecommunications and Media Informatics of the same university. He was a member of national research projects and the EFIPSANS, OPENLAB, UNIFY FP7 EU projects. His current research interests focus on Software Defined Networking, congestion control methods and autonomic computing.

András Gulyás received M.Sc. and Ph.D. degree in Informatics at Budapest University of Technology and Economics, Budapest, Hungary in 2002 and 2008 respectively. Currently he is a research fellow at the Department of Telecommunications and Media Informatics. His research interests are complex and self-organizing networks and software defined networking.

View-Invariant Person Identification by Orthogonal View Gait Signature and Fusion of Classifiers

Sagar Arun More, *Member, IEEE*, and Pramod Jagan Deore

***Abstract*—In this paper, we proposed the use of three orthogonal views of gait signature for view-invariant person identification system. We also experimented the fusions of classifiers in order to improve the recognition performance. Two classifiers used corresponding to two LDA spaces. The first classifier used for angle classification followed by second classifier for person identification. The proposed mechanism of selective kNN (s-kNN) has boosted the recognition performance and found very effective. We got 97.07% maximum rank-1 angle classification accuracy and 93% maximum rank-1 person identification accuracy.**

***Index Terms*—Gait Bio-metrics, View-Invariant, Linear Discriminant Analysis.**

I. INTRODUCTION

BIO-METRICS is considered as one of the successful applications of pattern recognition and has been widely used in several domains, such as authentication in highly restricted areas, attendance record in office premises, citizenship identification-verification and in the field of forensics. These bio-metric systems are mostly based on modalities like fingerprint, iris and face. However, commonly used bio-metric recognition systems usually operates in constrained acquisition scenarios and under rigid protocols. This scenario motivates researchers to explore the development of *non-cooperative* systems [1]. In the bio-metrics application which requires distant data (sample) capture, it becomes almost impossible to acquire the samples, e.g. fingerprints or iris. Besides popular bio-metric modalities like fingerprint, face and iris; activity based biometrics [2] can add the value to the identification process. Especially, in the case of bio-metric applications where far distant data capture process is involved. In such scenario, gait is the useful bio-metric trait. The gait recognition is based on the activity of person, namely walking. The gait activity is the composition of motion trajectories and coordinated movements of the various body parts and mostly suffer from the co-variate conditions.

There are several advantages of the gait based person identification over the conventional bio-metrics such as:

1) Most suitable for non-cooperative and unconstrained bio-metric process.
2) Walking normally happens with subject without demanding from it and hence it's a natural sample.
3) Unlike face and iris, gait can be captured from multiple angle / views, which makes data acquisition more informative.
4) Even works well with low quality video data.
5) No fine details are required as in face, iris or fingerprint based recognition system.

Though, the gait recognition has been researched for long time, there are challenges such as:

1) In some situations like restaurants, shopping malls walking doesn't always happen.
2) In crowded places, walking can be done in restrictive manner, leading to a change in gait cycle and affecting bio-metric process negatively.
3) Particular place or situation may have predictable activity to be happened more frequently and hence can be exploited e.g. in college / department canteen, shaking hands and paying bill after taking out wallet can be more dominant activities.
4) Gait sample may not give accurate shape profiles with loose clothes.
5) Gait can be affected by various co-variate factors like speed, cloths, surface of walking, illness, drunkenness, pregnancy.
6) Viewing angle effect plays vital role in multi view system.

In the unconstrained environment and distant data capture based bio-metric system, fingerprint, iris and face recognition could not be the right choice. Comparatively gait, comprised of motion trajectories of various body parts, have a potential to get captured properly from relatively far distance. It doesn't need systematic data capture process and only camera installation is required, where subjects are not necessarily be informed, which makes the identification process protocol free.

II. LITERATURE OVERVIEW

Gait recognition have attracted researchers in recent years because of it's various advantages as discussed earlier. The gait recognition methods can be broadly categorized as model free and model based methods. In model free methods, the features for recognition are directly extracted from the spatial domain and in model based methods the features are extracted by modelling the human body by some mathematical means.

a) Model Free Approach: This approach directly extract features from the spatial domain like [3], [4], which use Procrustes shape analysis. After extracting silhouette, authors apply Procrustes shape analysis to obtain mean shape as gait signature. Whereas in [5], gait energy image obtained

Sagar Arun More is with the Department of Electronics and Telecommunication Engineering, R. C. Patel Institute of Technology, Shirpur, 425405, INDIA e-mail: (sagar.more27@gmail.com).

Pramod Jagan Deore is with the Department of Electronics and Telecommunication Engineering, R. C. Patel Institute of Technology, Shirpur, 425405, INDIA e-mail: (pjdeore@yahoo.com).

Manuscript received; revised; accepted;.

from the sequence of gait images used for recognition as it preserves the temporal information. In [6], author use fusion of multiple gait cycles for recognition. The gait cycle is estimated by calculating auto correlation. From each gait cycle, they extract gait energy image and motion silhouette image for classification and recognition. The wavelet analysis is also used in gait recognition [7], [8]. In [7], author utilize the property of radon transform and Haar wavelet transform to extract horizontal and vertical features. Another wavelet based approach [8] use time-frequency analysis of extracted gait cycle. After wavelet decomposition they calculate mean, standard deviation, skewness and kurtosis of each sub-band. A simple city block distance measure is used for classification. Methods based on image geometry transformations have also been proposed [9], which is independent of view angle. In [10], author use height and stride length as soft bio-metrics in a probabilistic framework for gait recognition.

In a recent GEI based method [11], horizontal motion estimated by computing Shanon entropy of each row of GEI. Further, group Lasso learning algorithm is used to segment the motion based vector into blocks of similar motion values. The body part, which has highest average motion vector value is selected as a feature vector.

b) Model Based Approach: In this approach, the various features can be extracted by modelling human body. An initial model based attempt for gait-based recognition in a spatio-temporal (XYT) volume is done by Niyogi and Adelson [12]. A 5-stick model is used to generate gait pattern in XYT which is further used for classification. In [4], Procrustes analysis is used for static feature extraction and the dynamic features extracted by modelling the human body by truncated cone for various body parts and sphere for head. In [13], bulk motion, shape and articulated motion estimation was done by gait motion model adaptation. In [14], authors proposed a fusion based method, in which they divide silhouette into 7 parts and fit ellipse in those regions. They extract various parameters of ellipse. All these parameters of 7 regions constitute a novel feature vector. Whereas, [15] use fusion of several features for recognition like area, gravity center and orientation of each body part.

Recent development in model based gait recognition emphasizes modelling the multi-view gait sequences by using view normalization techniques. Worapan et al [16]–[19] use View Transformation Model (VTM) to normalize probe and gallery view in the same direction. The method presented in [16] is SVD based VTM approach and [17] is SVR based. The problem like data redundancy in their earlier methods is improved in [18]. Whereas, [19] uses MLP to construct VTM model for multi-view and cross-view gait recognition.

c) View-Invariant Approach: The view-invariant gait identification is relatively new research area. The most desirable property of this approach is to identify test subject walking at any arbitrary view angle. It uses either any one of two or both approaches as discussed earlier. i. e. model free or model based. In [20], a viewpoint independent method is proposed which requires single camera without calibration and prior knowledge of subject / person pose. The test subject is identified by projecting the limb motion of subject which is walking at arbitrary view angle onto the lateral / side-view plane. First, they do marker less joint estimation followed by reconstruction method for viewpoint rectification. In [21], author proposes a joint subspace learning method for view-invariant gait recognition. First, radon transform based energy images of sequences extracted and further they perform canonical correlation analysis to get representation coefficients, which they use as view-invariant features. Next, they obtain prototypes of various views by using PCA. The samples of different views represented as linear combination of these prototypes and then extract the coefficients which further used for recognition. Whereas in [22], author extracts a gait texture image which preserves gait information of a particular view angle. Further, they apply transform invariant low rank textures to project gait information of arbitrary view on to sagittal plane. In a recent paper [23], gait flow image extracted by Lukas-Kanade method as dynamic feature, head and shoulder mean shape by Procrustes shape analysis as static feature. In identification phase, they compute view angle or walking direction of test subject along with the static and dynamic features. A simple Euclidean distance classifier is used to find similarity measure between test and gallery images.

In [24], complete canonical correlation analysis is used to investigate correlation between two gait features considering normal walking sequences. They randomly select a sample for training and testing on different view angle. In [25], the authors extract width of 4 different sub regions of silhouette which then combined to construct gait signature. They considered all view angle and 3 normal walking sequences for training and each view angle taking one view at a time and 3 normal walking sequences for testing. A robust view invariant approach is proposed by [26], in which view angle is classified using entropy of the limb region of GEI and person identification is done by using multi scale shape analysis.

III. Overview of the Proposed Method

Gkalelis et. al. decomposes motion in activity as a combination of basic movement patterns, the so-called dynemes, calculated from fuzzy C-means (FCM) clustering method as described in [27]. The number of dynemes are decided from the leave-one-out cross-validation procedure, which is an extension of the method described in [28]. Their algorithm combines fuzzy vector quantization (FVQ) of [29] using posture vectors (column/row wise one-dimensional vector of binary silhouettes) and Linear Discriminant Analysis (LDA) to discover the most discriminating dynemes as well as represent and discriminate the different human movements in terms of these dynemes. This method was extended in [30], [31] and [32] for the multi-view videos. The training and testing videos were captured by multi-view cameras and dynemes were calculated from all the videos irrespective of their view angles to make the motion representation and their classification view independent.

Since, FCM or CM based clustering gives vector quantization of the posture vector description, it is possible that discriminative information may loss. This can be overcome using sparse coding of posture vectors as done in [33]. Hence, in this experiment, we use sparse coding of posture vector. The objective criterion and optimization of sparse coding were formulated as given in [34] and [35]. The results with mean and max pooling of feature representation from the sparse codebook were studied and found that, mean pooling based representation is most suitable. This approach compared with the large margin nearest neighbor (LMNN) [36] and found superior to it.

In this work, we use CASIA multi-view gait databases B [40] which consists of 124 subjects. Each subject is depicted in 10 instances (video sequences) with various co-variates like; normal/slow walking ($nm-01$ to $nm-06$), with bag ($bg-01$, $bg-02$), with coat ($cl-01$, $cl-02$). The instances are captured at 11 different viewing angles (0^o, ..., 180^o). Thus, the database consists of $124 \times 10 \times 11 = 13,640$ gait instances (video sequences). In this experiment, we use 6 instances i.e. normal and slow walking sequences.

We have experimented gait recognition using LDA with different number of training (K) and testing (S) sample's set (instances/sequences). The performance in form of recognition accuracy is shown in the Table I. Figure 1 shows it's graphical plot. It can be inferred that the reduction in the number of training samples generates over-fitting issue in the classifier and hence degrades the performance. Another hypothesis generated here by experimentation is that, performance with particular angle gait sequence is dependent on whether that angle samples are included in the training or not. In unconstrained environment, where subject is expected to walk in any direction yielding gait sequence in any angle, the issue of inclusion of particular angle becomes vital with two constraints. First, having the the number of all angle or regular discrete angles in the range of 0 to 180 degree in training can load the system resources like memory and computational power. Secondly, it can be unmanageable to capture gait sequences from subjects in all possible angle views. The performance across the possible angles with different set angles in training is shown in the Table II and Figure 2 shows it's plot. It is observed that, non-inclusion of particular angle-view gait sequences in training gives abrupt degradation by more than 90% fall in rank-1 accuracy. More recently there are some attempts as reported in [37], [38], [39] and [2], where classifier is trained with the set of instances which includes all the view angle sequences from each subject.

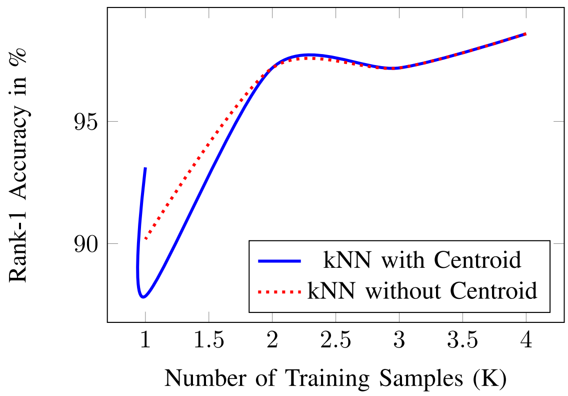

Fig. 1. Plot of Performance with different values of Training Samples -K (CASIA B)

IV. Proposed Methodology

The main complexity of the activity based recognition lies in three components, namely, 1) Dynemes Calculation, 2) Feature Extraction and 3) Classification. Our proposed approach use three orthogonal views in multi-view capture and sparse coding of posture vectors. The dynemes were used to calculate its histogram using distance measure and its fuzzification as described in [2]. The training features can be obtained by projecting training instances on the LDA subspace to maximize the discrimination in inter-class samples and minimize the intra-class variance. However, in doing so, kNN training instances with different gait-angles or view angles can give the enough variation in their features to overlap with space of other classes. To overcome this problem, we proposed to have two kNN classifiers corresponding to the two LDA subspaces in series. The first LDA subspace is to have projection from gait samples for discriminating them in different view-angle classes irrespective of the subject identity. The view angle is obtained from the first LDA subspace using kNN classifier trained by same training samples as used in dynemes calculation. The second LDA subspace, obtained with subjects classes irrespective of their view-angles (gait-angles), is then used to project gait samples for testing and training. The histogram features extraction and two LDA subspace construction are shown in Figure 3. While using kNN classifier on the test samples, test samples are compared only with the samples corresponding to the view angle obtained from angle based classifier. Thus, the kNN classifier selects the kNN samples from training instances based on the angle of the test gait sequence, as determined from the first classifier. This method is different from the framework proposed in [2] in the sense that, former employs the fusion of two classifiers in parallel, while later one uses two classifiers in series. However, the upper bound of performance in our approach is limited by the performance given by first classifier, which outputs the view-angle class and hence, it becomes critical component in the recognition system. This classifier is expected to give more than 95% performance in typical case, additionally its output decision can be validated by additional strategy. At present, this validation strategy is kept out of scope of this paper as angle identification classifier used here is certain to provide recognition accuracy of more than 97%. The system block diagram of our approach based on two classifiers in series is shown in Figure 4. The main contributions of this approach are,

1) This is most suitable for single-view camera with unconstrained gait sequence with respect to direction of walk.
2) The samples considered in person classifier are corresponding to the angle of gait sequence classified by angle classifier in which person is walking, as opposed to the all angle view inclusion in the person classifier before fusing the results as in case of [2].

Training Samples	Testing Samples	kNN with Centroid		kNN without Centroid	
K	S	Rank-1 Accuracy(%)	Avg. Accuracy(%)	Rank-1 Accuracy(%)	Avg. Accuracy(%)
[1,3,5,6]	[2,4]	98.59	97.65	98.59	97.65
[1,2,3,4]	[5,6]	96.72	97.65	96.72	97.65
[1,2,3]	[5,6]	94.85	96.37	95.32	96.49
[2,3,4]	[5,6]	96.72	96.37	96.26	96.49
[1,2,4]	[5,6]	96.72	96.37	97.19	96.49
[1,3,4]	[5,6]	97.19	96.37	97.19	96.49
[1,2]	[5,6]	94.39	96.37	94.39	96.49
[1,3]	[5,6]	94.39	96.37	95.32	96.49
[1,4]	[5,6]	97.19	95.32	97.19	95.47
[2,3]	[5,6]	94.85	95.32	94.39	95.37
[2,4]	[5,6]	95.79	95.32	95.79	95.47
[3,4]	[5,6]	95.32	95.32	95.79	95.47
[1]	[5,6]	87.85	90.18	87.85	90.18
[2]	[5,6]	90.18	90.18	90.18	90.18
[3]	[5,6]	88.78	90.18	88.78	90.18
[4]	[5,6]	93.92	90.18	93.92	90.18

TABLE I
PERFORMANCE WITH DIFFERENT TRAINING / TESTING SAMPLES SET OF CASIA B

Training with K=[1, 3, 5, 6]	% Testing Accuracy with S=[1, 2, 3, 4, 5, 6] with view angle as follows												Testing with Non-Ortho. View with S=[1to6]
View Angle	0^0	18^0	36^0	54^0	72^0	90^0	108^0	126^0	144^0	162^0	180^0	Avg. Accu.(%)	Avg. Accu.(%)
A=0	97.44	6.45	4.43	2.28	1.47	0.80	0.80	1.74	1.74	1.61	8.06	11.32	2.2
B=90	1.61	0.80	1.07	5.10	36.29	94.35	27.82	7.79	2.41	0.80	1.34	16.37	10.5
C=180	5.64	2.41	1.47	0.80	1.74	1.61	1.61	1.07	0.80	5.10	97.44	10.71	1.74
A+B+C	51.34	3.36	1.61	2.95	11.02	38.02	6.58	3.36	1.74	3.2	68.14	17.39	4.23
Min(A,B,C)	96.37	6.18	3.49	2.95	32.52	92.87	27.28	3.89	0.94	1.34	83.46	31.94	9.82

TABLE II
PERFORMANCE WITH ORTHOGONAL VIEW ANGLES 0^0, 90^0 & 180^0 TRAINING (CASIA B)

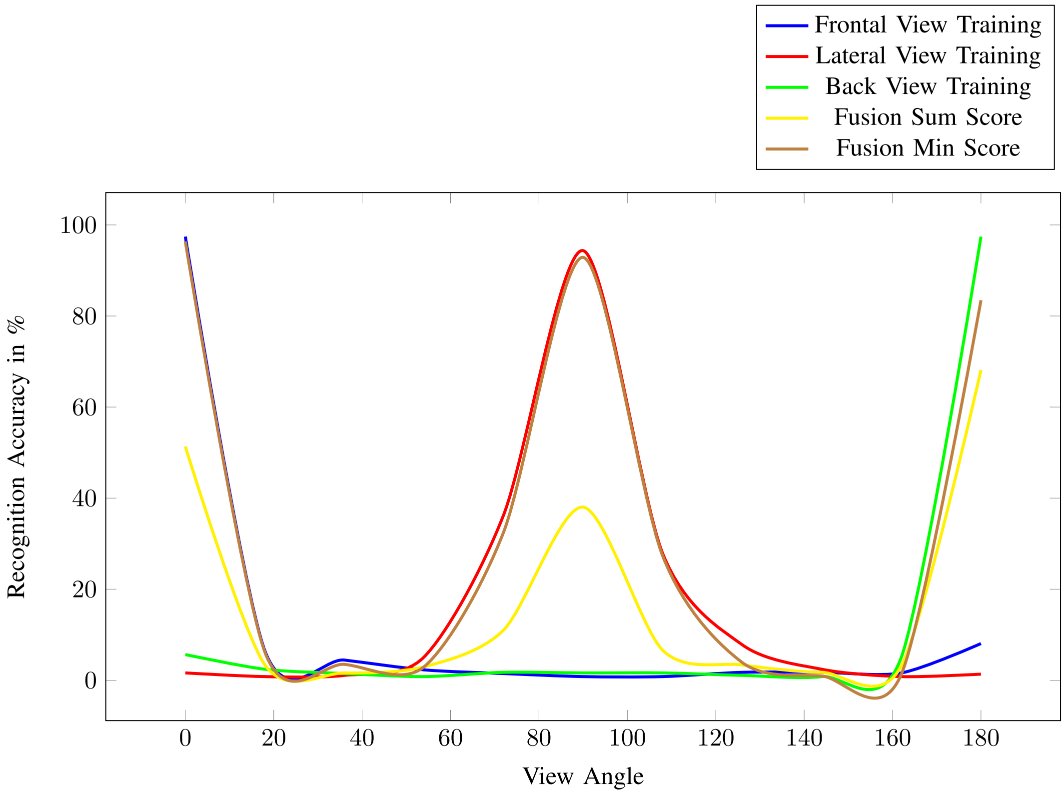

Fig. 2. Graph on Performance with Orthogonal View Angles 0^0, 90^0 & 180^0 Training (CASIA B)

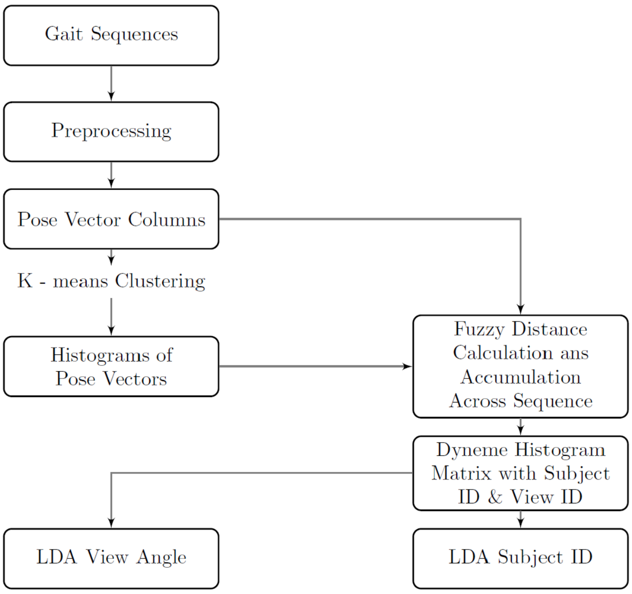

Fig. 3. Histogram Features Extraction and Two LDA Subspaces

3) The proposed mechanism of selective kNN (s-kNN) classifier improves the person identification result.
4) Significant results for non-orthogonal view angles.

The system with s-kNN i.e. rank-N s-kNN classifier is shown in Figure 5.

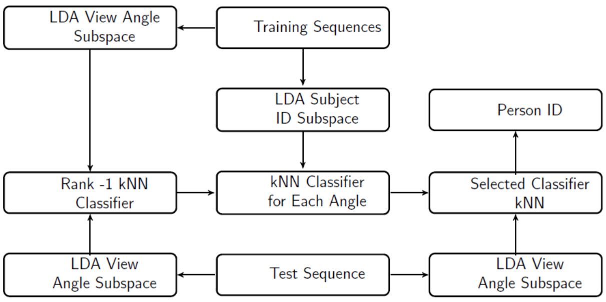

Fig. 4. S-kNN Classifier

V. Experimental Results and Discussion

Experiments performed considering normal and fast walking instances. Initially we performed experiment considering orthogonal angles 0^0, 90^0 & 180^0 in training instances $\{1, 3, 5, 6\}$ excluding instances $\{2, 4\}$. Results in terms of testing accuracy considering testing instances $\{1, 2, 3, 4, 5, 6\}$ is shwon in Table II. It is found that, the recognition accuracy infers when particular angle instance is not included in training. The average recognition accuracy for non-orthogonal view angles is also shown in Table II.

Experimentally it is found that, the orthogonal views of angles 18^0, 108^0 and 162^0 are useful for training efficiently as reported in [37]. As the dyneme representation is resilient

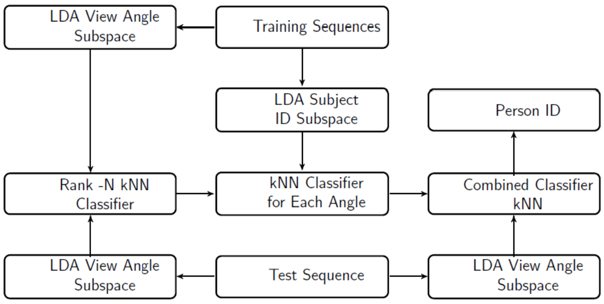

Fig. 5. Rank-N S-kNN Classifier

Fig. 6. Dynemes Poses

to noise, the set of 340 & 500 dynemes are calculated from training instances, $\{1, 3, 5, 6\}$ of 124 subjects with orthogonal view angles 18^o, 108^o and 162^o excluding instances $\{2, 4\}$. Figure 6 shows 500 dynemes for instances $\{1, 3, 5, 6\}$. The overall and across angle recognition accuracies are presented in Table III. The experiments were performed with LDA using kNN and s-kNN classifiers. Significant results obtained for non orthogonal view angles considering all instances by our method. Where, pID is person identification and VA is view angle accuracy.

The further improvement in the performance of system is achieved by rank-N s-kNN classifier. The results with different training set are shown in Table IV. It can be observed that, the rank-1 angle classification accuracy and pID rank-1 accuracy improves significantly with increased number of instances in training.

A. Comparative Work

In [37], the strategy was proposed to determine the least number of viewing angles from available maximum number of views to be used in training so that recognition with different gait angle sequences can be maximized. It is the optimization problem and training set with views from 18^o, 108^o and 162^o is experimentally found to be the best solution. We implemented our approach with these training set and compared with results obtained with their approach as reported

Training with K=[1, 3, 5, 6] with 124 Sub.	Testing % Accuracy with S=[1, 2, 3, 4, 5, 6] with view angles as follows											Testing with Non-Ortho. Views with S=[1 to 6]
	0^0	18^0	36^0	54^0	72^0	90^0	108^0	126^0	144^0	162^0	180^0	Avg.%
340-LDA-kNN	95.83	96.23	95.56	94.62	87.76	85.61	87.09	92.33	93.81	93.27	95.56	92.52
500-LDA-kNN	95.16	96.37	96.63	95.29	88.97	85.88	89.65	94.48	94.48	93.95	96.10	93.36
340-LDA-S-kNN	97.58	97.31	96.10	96.63	94.62	89.65	91.66	95.43	94.48	93.27	96.77	94.85-pID
340-LDA-S-kNN	97.84	98.25	97.44	97.17	97.71	97.58	6.10	96.50	94.75	94.35	97.58	96.84-VA
500-LDA-S-kNN	97.17	97.58	96.50	96.77	94.22	89.51	93.01	95.56	94.35	93.95	97.74	95.06-pID
500-LDA-S-kNN	97.84	98.92	97.17	97.04	97.84	97.98	96.23	96.50	94.75	94.35	97.71	95.94-VA

TABLE III
PERFORMANCE WITH LDA USING KNN AND S-KNN CLASSIFIERS WITH NO. OF DYNEMES 340 AND 500 TRAINED BY ORTHOGONAL VIEW ANGLES 18^0, 108^0 & 162^0 (CASIA B)

Training and Testing Sets 124 Subjects	Rank-1 Angle Classification Accuracy		Person ID-Rank - 1 Accuracy(%) with Different S and K with Rank - N Classification where N is as follows										
K and S Sets	Testing Sample	Rank-1 Angle Accu. %	1	2	3	4	5	6	7	8	9	10	11
K=[1], S=[2, 3, 4, 5, 6]	6660	6366 (95.58)	64.09	64.09	64.81	64.86	64.83	64.87	64.90	64.89	64.87	64.86	64.81
K=[1, 3] S=[2, 4, 5, 6]	5321	5118 (96.18)	78.81	78.18	79.57	79.64	79.74	79.75	79.75	79.79	79.81	79.39	79.92
K=[1, 3, 5] S=[2, 4, 6]	3991	3861 (96.73)	87.59	87.59	88.37	88.49	88.62	88.67	88.79	88.82	88.79	88.82	88.84
K=[1, 3, 5, 6], S=[2, 4], 124/104 Subjects	2675 /2341	2592 (96.89) /2287 (97.68)	91.25 /92.39	91.25 /92.39	92.07 /92.95	92.26 /92.99	92.29 93.03	92.33 93.07	92.37 /93.07	92.33 93.07	92.33 /93.07	92.33 /93.07	92.29 93.07
K=[1, 2, 3, 5, 6],S=[4]	1329	1290 (97.07)	93.00	93.00	93.22	93.52	93.60	93.82	93.82	93.90	93.90	93.90	93.90

TABLE IV
RANK-1 ACCURACY OF PERSON IDENTIFICATION WITH DIFFERENT SETS OF K AND S WITH RANK-N CLASSIFIER FOR ORTHOGONAL VIEWS 18^0, 108^0 & 162^0 (CASIA B)

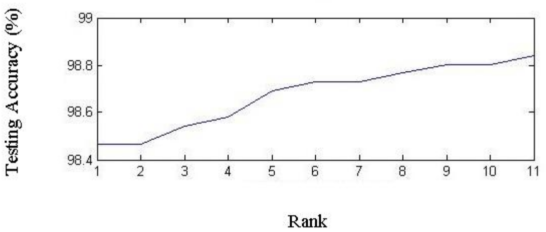

Fig. 7. Testing Accuracy of Angle Classifier for angle 180^0

in the Table V. It can be seen that, our approach gives slightly improved performance over this method.

In [39], the correlation motion analysis for each point in GEI is done across the views and the sparse regression is carried out with the help of correlation coefficient. Once the regression GEI features across any view-angle is obtained, the view classifier estimates the angle of test gait sequence walked in any direction. This classifier is based on the GEI features projected on the PCA and later PCA transformed features are used in constructing LDA subspace. Using projection of training images in LDA subspace to compare with that of test images, angle is estimated. This step is similar to angle based classifier used in our algorithm, with only difference of using dynemes histogram as a features in place of GEI features and using LDA subspace directly instead in PCA transformed space. In this approach, sparse regressive GEI data corresponding to the estimated angle refined by ROI selection based on motion correlation is used in classifier after projecting it on PCA. The Euclidean distance as a similarity measure, is used in the classifier for identifying the person. We have compared our approach with this method reported in [39]. To be fair with comparison, we used first 24 classes to make the dynemes model and remaining 100 classes used for view-angle classification and person identification as specified in their work. Figure 7 shows testing accuracy of angle classifier for angle 180^0. From the results it can be seen that, our approach outperforms almost at every place. The variant of this

Training with K=[1, 3, 5, 6] with 124 Sub.	Testing Accuracy with (S=[2, 4])		Testing Accuracy(%) with S=[2, 4] with view angle as follows										
	Correct	% Accu.	0^0	18^0	36^0	54^0	72^0	90^0	108^0	126^0	144^0	162^0	180^0
Method [37]	-	90.72	87.9	96.37	94.35	87.1	84.68	91.94	97.18	88.31	87.9	97.18	85.08
Proposed Method	2425	91.25	94.67	95.93	92.68	95.49	86.53	73.06	84.08	95.85	95.78	92.85	97.13

TABLE V
COMPARISON WITH METHOD [37]

Training with K=[1, 3, 5, 6] with 124 Sub.	Testing Accuracy with (S=[2, 4])		Testing Accuracy(%) with S=[2, 4] with view angle as follows											Avg. Accu.(%)
	Correct	% Accu.	0^0	18^0	36^0	54^0	72^0	90^0	108^0	126^0	144^0	162^0	180^0	
Method [39]	-	90.5	88			95		88		91				90.5-pID
			90	91	91	98	99	91	93	94	92	93	91	94-VA
Proposed Method	1971	92.22	91.41	94.94	95.45	95.91	92.38	77.15	85.27	95.87	96.82	93.26	95.91	92.22-pID
			98.86	98.98	96.96	95.42	98.98	94.41	94.41	100	97.35	94.81	98.46	97.22-VA

TABLE VI
COMPARISON WITH METHOD [39]

work is also presented in [38] using different type of regression method to select the optimized feature representation.

In [2], authors proposed the framework for person identification based on various activities like; jump in place, wave one hand, jump forward, run, walk (gait). Although, we focused on gait activity only. The features extracted in [2] are the histogram of dynemes (centroid of clusters) calculated and accumulated from each of the frame throughout the video sequence. This algorithm doesn't need to calculate the gait cycle and thus it is shift invariant in time. Two subspaces are created using LDA from the dynemes histogram features. One for subject class and another for view-angle. The kNN classifier with centroid is applied to each of the view of probe subject to decide its view angle and its subject class. These two labels obtained from N camera views are fed to the Bayesian Framework to obtain final output in terms of person class. It is important to mention here that our feature extraction method is very much adopted from this work because of its shift-invariant property. It can also be used for continuous person identification. However, the classification strategy used in our approach is hard than the one used in [2]. We compared our algorithm with the results provided in this paper. The experiment includes the 5 sample instances as training and testing is done on remaining one instance as mentioned in [2]. The recognition accuracy is reported in this paper is 93.27%, while our approach gives the accuracy of 94.19%. This shows the slight improvement can be gained with our approach.

VI. CONCLUSION

We have explored the view-invariant gait recognition system which use three orthogonal views of gait signature for the person identification. It is observed that, training with orthogonal views becomes very effective in multi-view gait recognition. Another proposed mechanism of selective kNN (s-kNN) to fuse the two classifiers have been successful in improving the gait recognition accuracy. Initially, we performed experiment considering orthogonal angles 0^0, 90 and 180^0. It is observed that, the recognition accuracy decreases abruptly if test instance of a particular view angle not included in training. The testing accuracy for non-orthogonal view angle was also infer. Next, we use optimized view angle framework with orthogonal view angles 18^0,108^0 and 162^0 for training. Various experiments were performed considering 340 and 500 dynemes for kNN and s-kNN classifier. We got significantly improved results even for non-orthogonal view angles. We report 97.07% maximum rank-1 angle classification accuracy and 93% maximum rank-1 person identification with different sets of K and S for rank N s-kNN classification. It is observed that s-kNN perform better than kNN in pID (person identification) and VA (view angle accuracy).

ACKNOWLEDGMENT

Portions of the research in this paper use the CASIA Gait Database collected by Institute of Automation, Chinese Academy of Sciences. The authors are grateful to anonymous reviewers for their critical suggestions and comments which greatly helped in improving the quality and presentation of the paper. Authors are also grateful to Prof. Yogesh Ratnakar Vispute for proof reading of the paper.

REFERENCES

[1] M. Savvides, K. Ricanek, D. L. Woodard, and G. Dozier, "Unconstrained Biometric Identification: Emerging Technologies," *Computer*, vol. 43, pp. 56–62, 2010.

[2] A. Iosifidis, A. Tefas, and I. Pitas, "Activity-Based Person Identification using Fuzzy Representation and Discriminant Learning," *IEEE Transactions on Information Forensics and Security*, vol. 7, no. 2, pp. 530–542, 2012.

[3] Liang Wang, Tieniu Tan, Weiming Hu, and Huazhong Ning, "Automatic Gait Recognition Based on Statistical Shape Analysis," *IEEE Transactions on Image Processing*, vol. 12, no. 9, pp. 1120–1131, 2003.

[4] L. Wang, H. Ning, T. Tan, and W. Hu, "Fusion of Static and Dynamic Body Biometrics for Gait Recognition," *IEEE Transactions on Circuits and Systems for Video Technology*, vol. 14, no. 2, pp. 149–158, 2004.
[5] J. Han and B. Bhanu, "Individual Recognition using Gait Energy Image." *IEEE Transactions on Pattern Analysis and Machine Intelligence*, vol. 28, no. 2, pp. 316–322, 2006.
[6] S. H. S. Hong, H. L. H. Lee, and E. K. E. Kim, "Fusion of Multiple Gait Cycles for Human Identification," *2009 ICCAS-SICE*, pp. 3171–3175, 2009.
[7] H. Z. H. Zhang and Z. L. Z. Liu, "Gait Representation and Recognition Using Haar Wavelet and Radon Transform," *WASE International Conference on Information Engineering*, vol. 1, pp. 83–86, 2009.
[8] T. Amin and D. Hatzinakos, "Wavelet Analysis of Cyclic Human Gait For Recognition," *Sixteenth International Conference on Digital Signal Processing*, pp. 1–6, 2009.
[9] H. Su and G. Y. Chen, "A New Method of Gait Recognition Independent of View Angle," *International Conference on Machine Learning and Cybernetics, ICMLC*, vol. 6, pp. 3091–3096, 2010.
[10] K. Moustakas, D. Tzovaras, and G. Stavropoulos, "Gait Recognition Using Geometric Features and Soft Biometrics," *IEEE Signal Processing Letters*, vol. 17, no. 4, pp. 367–370, 2010.
[11] G. M. Imad Rida, Xudong Jiang, "Human Body Part Selection by Group Lasso of MotionforModel-FreeGaitRecognition ," *IEEE Signal Processing Letters*, vol. 23, no. 1, pp. 154–158, 2016.
[12] S. A. Niyogi and E. H. Adelson, "Analyzing and Recognizing Walking Figures in XYT," *Conference on Computer Vision and Pattern Recognition, CVPR*, pp. 469–474, 1994.
[13] D. K. Wagg and M. S. Nixon, "On Automated Model-based Extraction and Analysis of Gait," *Sixth IEEE International Conference on Automatic Face and Gesture Recognition*, pp. 11–16, 2004.
[14] L. Lee and W. E. L. Grimson, "Gait Analysis for Recognition and Classification," *Proceedings of Fifth IEEE International Conference on Automatic Face Gesture Recognition*, pp. 734–742, 2002.
[15] N. V. Boulgouris, "Model-based Human Gait Recognition using Fusion of Features," *IEEE International Conference on Acoustics Speech and Signal Processing (2009)*, pp. 1469–1472, 2009.
[16] H. L. Worapan Kusakunniran, Qiang Wu and J. Zhang1, "Multiple Views Gait Recognition using View Transformation Model Based on Optimized Gait Energy Image ," *In Proc.* 12^{th} *IEEE International Conference on Computer Vision*, pp. 1058–1064, 2009.
[17] ——, "Support Vector Regression for Multi-View Gait Recognition based on Local Motion Feature Selection ," *In Proc. IEEE Conference on Computer Vision and pattern Recognition*, pp. 974–981, 2010.
[18] ——, "Gait Recognition Under Various Viewing Angles Based on Correlated Motion Regression ," *IEEE Transaction on Circuits and Systems for Video Technology*, vol. 22, no. 6, pp. 966–980, 2012.
[19] H. L. Worapan Kusakunniran, Qiang Wu and J. Zhang, "Cross-view and Multi-view Gait Recognitions based on View Transformation Model using Multi-Layer Perceptron ," *Pattern Recognition Letters*, vol. 33, no. 7, pp. 882–889, 2012.
[20] M. Goffredo, I. Bouchrika, J. N. Carter, and M. S. Nixon, "Self-Calibrating View-Invariant Gait Biometrics." *IEEE Transactions on Systems Man and Cybernetics: Part B Cybernetics*, vol. 40, no. 4, pp. 997–1008, 2010.
[21] N. Liu, J. Lu, and Y. P. Tan, "Joint Subspace Learning for View-Invariant Gait Recognition," *IEEE Signal Processing Letters*, vol. 18, no. 7, pp. 431–434, 2011.
[22] W. Kusakunniran, Q. Wu, J. Zhang, and H. Li, "A New View-Invariant Feature for Cross-View Gait Recognition," *IEEE Transaction on Information Forensic and Security*, vol. 8, no. 10, pp. 1642–1653, 2013.
[23] S. Jia, L. Wang, and X. Li, "View-Invariant Gait Authentication Based on Silhouette Contours Analysis and View Estimation," *IEEE/CAA Journal of Autometica Sinica*, vol. 2, no. 2, pp. 226–232, 2015.
[24] T. Y. Z. L. Xianglei Xing, Kejun Wang, "Complete Canonical Correlation Analysis With Application to Multi-View Gait Recognition," *Pattern Recognition, Elsevier B. V.*, no. 50, pp. 107–117, 2016.
[25] W. Zeng and C. Wang, "View- Invariant Gait Recognition Via Deterministic Learning," *Neurocomputing, Elsevier B.V.*, no. 175, pp. 324–335, 2016.
[26] T. T. Sruti Das Choudhury, "Robust View-Invariant Multiscale Gait Recognition ," *Pattern Recognition Letters*, vol. 48, no. 3, pp. 798–811, 2015.
[27] N. Gkalelis, A. Tefas, and I. Pitas, "Combining Fuzzy Vector Quantization with Linear Discriminant Analysis for Continuous Human Movement Recognition," *IEEE Transactions on Circuits and Systems for Video Technology*, vol. 18, no. 11, pp. 1511–1521, 2008.
[28] M. Zhu and A. Martinez, "Subclass Discriminant Analysis," *IEEE Transactions on Pattern Analysis and Machine Intelligence*, vol. 28, no. 8, pp. 1274 –1286, 2006.
[29] N. Karayiannis and P.-I. Pai, "Fuzzy Vector Quantization Algorithms and Their Application in Image Compression," *IEEE Transactions on Image Processing*, vol. 4, no. 9, pp. 1193 –1201, 1995.
[30] A. Iosifidis, N. Nikolaidis, and I. Pitas, "Movement Recognition Exploiting Multi-View Information," *IEEE International Workshop on Multimedia Signal Processing (MMSP), 2010*, pp. 427 –431, 2010.
[31] A. Iosifidis, A. Tefas, and I. Pitas, "Person Specific Activity Recognition using Fuzzy Learning and Discriminant Analysis," *Euripean Signal Processing Conference (EUSIPCO)*, 2011.
[32] A. Iosifidis, A. Tefas, N. Nikolaidis, and I. Pitas, "Multi-view Human Movement Recognition based on Fuzzy Distances and Linear Discriminant Analysis," *Computer Vision and Image Understanding*, vol. 116, no. 3, pp. 347 – 360, 2012.
[33] J. Lu, J. Hu, X. Zhou, and Y. Shang, "Activity-based Person Identification using Sparse Coding and Discriminative Metric Learning," *20th ACM international conference on Multimedia*, pp. 1061–1064, 2012.
[34] J. Yang, K. Yu, Y. Gong, and T. Huang, "Linear Spatial Pyramid Matching using Sparse Coding for Image Classification," *IEEE Conference on Computer Vision and Pattern Recognition, 2009*, pp. 1794–1801, 2009.
[35] H. Lee, A. Battle, R. Raina, and A. Y. Ng, "Efficient Sparse Coding Algorithms," *Advances in Neural Information Processing Systems*, pp. 801–808, 2007.
[36] N. Gkalelis, A. Tefas, and I. Pitas, "Human Identification from Human Movements," *16th IEEE International Conference on Image Processing (ICIP), 2009*, pp. 2585 –2588, 2009.
[37] N. Liu and Y.-P. Tan, "View Invariant Gait Recognition," *IEEE International Conference on Acoustics Speech and Signal Processing (ICASSP)*, pp. 1410–1413, 2010.
[38] S. Zheng, J. Zhang, K. Huang, R. He, and T. Tan, "Robust View Transformation Model for Gait Recognition," *18th IEEE International Conference on Image Processing (ICIP)*, pp. 2073–2076, 2011.
[39] W. Kusakunniran, Q. Wu, J. Zhang, and H. Li, "Gait Recognition Under Various Viewing Angles Based on Correlated Motion Regression," *IEEE Transactions on Circuits and Systems for Video Technology*, vol. 22, no. 6, pp. 966–980, 2012.
[40] S. Zheng, J. Zhang, K. Huang, R. He, and T. Tan, "Robust View Transformation Model for Gait Recognition," *International Conference on Image Processing(ICIP)*, 2011.

Sagar Arun More was born in Maharashtra, India. He received B.E. degree in Electronics from the North Maharashtra University, Jalgaon, India, in 2000 and the M. E. degree in Electronics from Sant Gadage Baba Amravati University, Amravati, India, in 2008. He is currently pursuing Ph.D. from North Maharashtra University Jalgaon. He current research interests include image and video processing, biometrics.

Pramod Jagan Deore was born in Maharashtra, India. He received the B. E. degree in Electronics from the North Maharashtra University, Jalgaon, India, in 1997.He received the M. E. and Ph.D. degrees from SGGS Institute of Engineering and Technology, Swami Ramanand Teerth Marathwada University, Nanded, in 1999 and 2007 respectively.
He is Professor of Electronics and Telecommunication Department at the R. C. Patel Institute of Technology, Shirpur, India. His research interests include Interval arithmetic operations applications in robust control, Image processing, and Bio-medical signal processing, Microwave circuits and antennas etc. He has published 40 papers in National/International Conferences/Journals and he has Co-authored two books. He is life member of ISTE.

Live Face Detection Method Based on Local Binary Pattern and Bandelet

Haiqing Liu, Shuhua Hao, Yuancheng Li, Xiang Li and Jie Ma

***Abstract* —Face recognition system is exposed to video replay attacks and photo spoofing attacks along with the extensive use of identity authentication technology. Spoofing attack happens when an attacker tries to disguise as a legitimate user with permissions to spoof authentication system by replaying the recorded videos of legitimate users or utilizing the printed photos of legitimate users. Inspired by the differences between image acquisition and playback, printing properties, and light emission models, this paper proposes a live face detection method based on local binary pattern and Bandelet. The replayed video images and the printed face images usually contain characteristics that are easy to be detected by texture detection and frequency domain analysis. The proposed method analyzes the differences between live faces and photo faces in texture, at the same time it utilizes Bandelet to analyze face images with multi-scale analysis and extracts the high-frequency sub band coefficients as feature vectors to train Extreme Learning Machine (ELM) to classify and recognize. The algorithm is verified on the public CASIA_FASD, print-attack and replay-attack datasets, well known Face Anti-Spoofing Databases, and the experimental results show that the method reduces the computational complexity and improves the detection accuracy.**

Index Terms*—*liveness detection; Bandelet transform; replay attack; authentication technology

I. INTRODUCTION

IN recent years, biometric authentication has attracted more and more attention, such as the safety assessment and vulnerability assessment. As a convenient user authentication technology, face recognition only needs regular cameras and a face detection application, so it has been widely applied to various scenarios under the efforts of many researchers. To give some examples, we can mention entrance guard systems, access security checks, criminal detection, the banking system, etc. However, face recognition system detects human faces through the analysis of the tactic flat images, so the system is easy to be spoofed by replayed videos or printed photos. In a real application scenario, the identity authentication system mainly faces three common spoofing methods [1].

1) Photo spoofing [2]: It is one of the most convenient spoofing methods to access the photos of legitimate users. The spoofer bends and rotates the printed photos in front of image acquisition devices to simulate the real legitimate users, which can spoof the authentication system.

2) Video spoofing [3]: The video of legitimate users is a more threatening spoofing tool, and it can be acquired by the secret cameras. Compared with photos, videos have characteristics of head movements, facial expressions, blink, etc. and their effects are similar to the real human faces.

3) 3D model spoofing: Make a 3D model for the human faces of legitimate users, which can simulate the blink, talking, head movements of real people [2-4]. Compared with the photo spoofing and video spoofing, 3D model spoofing is more threatening, but forging the live 3D model is more difficult. So, photo spoofing and video spoofing are the most used methods of identity authentication spoofing.

In this paper, our goal is to use a better algorithm to distinguish between real and fake faces. We propose a novel live face detection method, based on local binary pattern and Bandelet that extracts texture features from living bodies and photos, and then trains ELM classifier to identify authenticity. Finally, the result is verified on the public CASIA_FASD database, print-attack and replay-attack databases. Our experimental results show that the proposed algorithm performs well on all datasets.

The contribution of this article can be summarized as follows. We proposed a fusion method of LBP and Bandelet algorithm for countering spoof attacks in face recognition. We optimize the basic LBP and Bandelet algorithm to extract the features from face image respectively. Then we fuse the features and put them into the ELM classifier for training and learning. Our method finally is verified and evaluated on public CASIA-FASD, print-attack and replay-attack datasets, and the results show that the proposed approach outperforms the other methods in spoof detection.

The rest of this paper is organized as follows: Section II presents related works about face spoofing detection. Section III introduces the details of our live face detection method, the local binary pattern, Bandelet decomposition, and the ELM classifier. Section IV shows our experimental results. Finally, we conclude the paper in section V.

II. RELATED WORKS

Currently, many scholars in China and the rest of the world are committed to the study of the liveness detection problem, and there are already many live detection methods that are presented in the international conferences and journal articles. Presently, the live detection methods applied to face recognition mainly include the following categories:

This work was supported in part by the Scientific Research Foundation for the Returned Overseas Chinese Scholars, State Education Ministry ([2013]693).

All the authors come from the school of Control and Computer Engineering in North China Electric Power University.

Haiqing Liu (email: hqliu@ncepu.edu.cn), Shuhua Hao (email: shhao@ncepu.edu.cn (new), hsh0218hsh@163.com (old)) . Yuancheng Li (Corresponding author, Email: ycli@ncepu.deu.cn).

A. Image quality analysis based methods

As an example of image quality analysis method, D. Gong et al. proposed a new feature descriptor called common encoding model for heterogeneous face recognition, which is able to capture common discriminant information, such as the large modality gap [5]. I. Kim proposed a novel approach to robustly find the spoofing faces using the highlight removal effect, which is based on the reflection information. Because the spoofed face image is recaptured by a camera, it has additional light information [6]. D. Wen et al. proposed an efficient and rather robust face spoof detection algorithm based on image distortion analysis (IDA). Four different features (specular reflection, blurriness, chromatic moment, and color diversity) are extracted to form the IDA feature vector [7]. M. Uzair et al. proposed a hyperspectral face recognition algorithm using a spatiospectral covariance for band fusion and partial least square regression for classification. Moreover, they extended 13 existing face recognition techniques, for the first time, to perform hyperspectral face recognition [8]. Galbally et al. extracted 25 features from an image such as peak signal-to-noise ratio and structural similarity index to detect subtle image quality [9]. Karubgaru et al. solved the feature extracted method by "increasing" the data available from the original image using several preprocesses, such as, image mirroring, colour and edges information [10].

B. Move option based methods

Shervin et al. proposed a multiscale dynamic texture descriptor based on binarized statistical image features on three orthogonal planes (MBSIF-TOP) that is effective in detecting spoofing attacks and showing promising performances compared with existing alternatives [11]. Pan et al. have conducted live detection by blink actions [12]. Santosh T et al. have proposed a classification pipeline consisting of DMD, local binary patterns (LBPs), and support vector machines (SVMs) with a histogram intersection kernel. A unique property of DMD is its ability to conveniently represent the temporal information of the entire video as a single image with the same dimensions as those images contained in the video [13]. W. Yin et al. explored the issue of face anti-spoofing with good performance in accuracy by utilizing optical flow vector on two types of attacks: photos and videos shown on high-resolution electronic screens. The key idea is to calculate the displacement of the optical flow vector between two successive frames of a face video and obtain a displacement sum of a certain number of frames [14]. Many scholars were studying video sequences and dynamic descriptors that were extracted from video sequences [15-16]. Besides, Zhang Yu et al. improved the Piecewise Aggregate Approximation (PAA) method, and proposed a Hierarchical Clustering technique (HC-PAA) [17].

C. Texture based methods

N. Werghi et al. presented a novel approach for fusing shape and texture local binary patterns (LBPs) on a mesh for 3D face recognition. Using a recently proposed framework, they computed LBP directly on the face mesh surface, then they construct a grid of the regions on the facial surface that can accommodate global and partial descriptions [18]. K. Patel et al. analyzed the image distortion of the print and replay attacks using different: 1) intensity channels (R, G, B, and grayscale); 2) image regions (entire image, detected face, or facial component between nose and chin); and 3) feature descriptors. They developed an efficient face spoof detection system on an Android smartphone. Their studies of Android face spoof detection system involving 20 participants showed that the proposed approach worked very well in real application scenarios [19]. Pereira et al. applied a local binary pattern (LBP) to the X-Y，X-T and Y-T dimensions to analyze the texture of time and space [20]. T. Edmunds et al. proposed an original approach was that the fake face detection process occurs after the face identification process. Having access to enrollment data of each client, it becomes possible to estimate the exposure transformation between a test sample and its enrollment counterpart [21].

Table I Comparative of different face spoof detection methods

Type	Mechanism	Strengths	Limitations
Image quality analysis [5-10]	Image quality analysis of different attack image	Good generalization ability Fast response	Different classifiers needed for different spoof attacks
Move option [11-17]	Get the dynamic description in the video sequence	Good generalization ability	Slow response High computational complexity
Texture [18-21]	Analyze image static texture information	Fast response Low computational complexity	Vulnerable to the variations in acquisition conditions

Although much work has been directed towards tackling issues related to face spoofing detection, there is still significant room for improvement for anti-spoofing methods in face recognition [22]. Table I shows some advantages and disadvantages of the three methods listed in this article. In this paper, we proposed live face detection method based on local binary pattern and Bandelet. This method doesn't need users' active cooperation, so it has certain concealment. At the same time, the dimensions of extracted features are not high, while it reduces the time and the algorithm complexity.

III. LIVE FACE DETECTION METHOD BASED ON MULTISCALE ANALYSIS

It could be very difficult for us to distinguish the live faces in the photos accurately with our eyes, as shown in Figure I. In fact, live faces are complicated non-rigid 3D objects, while photo faces or video faces are flat rigid objects, so they can differ in light reflection and shadow. Photo faces usually contain the defects of printing quality, and this difference can be detected well by utilizing texture details.

A. Local Binary Pattern

Local binary pattern is a kind of operator used to describe the local texture features of images. Obviously, its function is feature extraction, and the extracted features are the texture features of images and they are local texture features. As show in Figure II, the original LBP operator is defined in the window of 3x3 pixels. The window's center pixel is regarded as a threshold and is compared with the grey values of eight adjacent pixels. If the surrounding pixel value is greater than the center pixel value, then the position of this pixel is marked as 1, otherwise is marked as 0. In this case, eight points in a 3x3 window can produce an 8-bit unsigned number, and then the LBP value of this window can be obtained to reflect the texture information of this area.

Figure I. Live faces in the CASIA database (a), photo faces (b) and video faces (c).

After the original LBP was brought up, researchers increasingly proposed various improvements and optimizations to get an LBP operator where there are P sampling points in the circular area with R in radius: LBP uniform pattern, LBP rotation invariant pattern, LBP equivalent pattern, etc.

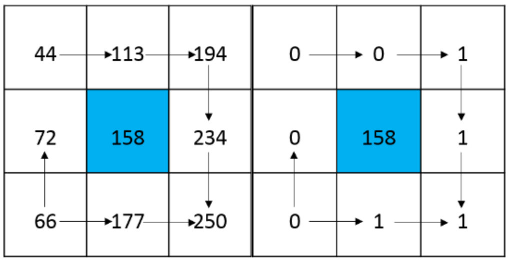

Figure II. The processing of LBP

Apparently, the above extracted LBP operator can get an LBP code in each pixel. Then, the obtained original LBP features are still an image after extracting the original LBP operator from an image. However, the objects in this image have been converted to secondary features, which cannot be directly applied to the discriminant analysis. We can see that this feature is closely relevant to the position information from the above analysis. So it can have a considerable deviation due to non-aligned positions if we directly conduct discriminant analysis on this feature of two images. Later, the researchers found that an image can be divided into several sub areas and LBP features are extracted from each pixel in each sub area, and then, statistical histograms of LBP features are established in each sub area. In this way, each sub area can be described by a statistical histogram. The whole image is composed of several statistical histograms. For example, an image with 100x100 pixels is divided into 100 sub areas with 10x10 pixels, and the size of each sub area is 10x10 pixels. LBP features are extracted from each pixel in each sub area, and then, statistical histograms are established. In this way, the image has 10x10 sub areas and 10x10 statistical histograms. This image can be described by these 10x10 statistical histograms. After that, we can judge the similarity between two images by various similarity measure functions.

At present, the LBP local texture extraction operator has been successfully applied to fingerprint recognition, character recognition, face recognition, license plate recognition and other fields.

B. Bandelet Decomposition

The main idea of constructing Bandelet transform [23] is to define geometric features in images as a vector field, rather than a set of common edges. And the vector field denotes the local regularity direction of gray value variations in an image spatial structure. Bandelet base is not predetermined, and it is chosen according to the optimization of final application results. A. Lutz et al. proposed the quick search method of the optimal base in Bandelet variation.

For geometric regularity images, geometric flows are parallel within a local scope. The wavelet transform is essentially the convolution of wavelet function and the original image, and the wavelet function can be regarded as the fuzzy kernel in this sense, so wavelet transform has a smoothing effect on the original image. This smoothing effect makes the image to has the regularity of direction that is vertical with the geometric flow, and it makes that the positioning of geometric flow doesn't need to be strictly accurate, being allowed to have a certain deviation. In view of the difficulties of accurate positioning of image edge line, this regularity makes it convenient to position geometric flow rapidly.

Image segmentation adopts the binary segmentation method which Donoho adopted in wedgelet. Firstly, a square image is equally divided into 4 sub areas, and then, each sub area is equally divided into 4 sub areas in the next layer of segmentation, until the size of sub areas at the bottom layer reaches the minimum preset. The segmentation result can be shown by quadtree; each sub area corresponds to one node of the quadtree, as shown in Figure III. When the width of an image is 1, and the width of the sub area is $(1/2)^{-n}$, the depth of the quadtree node corresponding to the sub area is n.

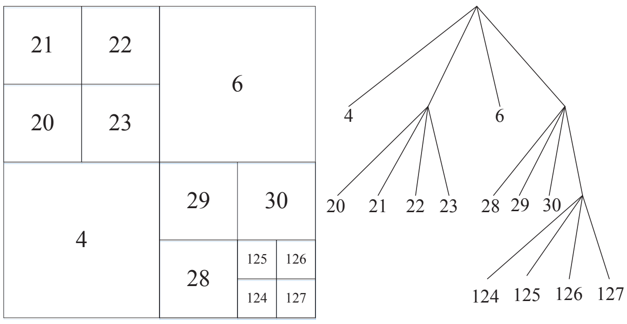

Figure III. Binary tree decomposition diagram

C. The Proposed Live Face Detection Method

As for texture feature detection, this paper proposes a live face detection method based on LBP and Bandelet to solve this problem. The flowchart of this method is shown in Figure IV.

Step 1 Convert the face image to be detected into a grayscale image, remove the redundant color information and keep the texture information.

Step 2 Extract the local binary pattern features and statistical features of high-frequency coefficients in Bandelet transform from the converted grayscale image.

The process of getting local binary pattern features is:
1) Divide the detected window into several sub areas (for example, the size of every sub area is 16x16 pixels).
2) Compare every pixel in the sub areas with its eight neighborhood pixels (upper left, left middle, lower left, upper right, etc.), which can be carried out in accordance with the clockwise or counter-clockwise order.
3) If the surrounding pixel value is greater than the center pixel value, then the position of this pixel is marked as 1, otherwise, is marked as 0. In this case, an 8-bit binary number is obtained and converted to a decimal number to be as the feature of this area.
4) Establish histograms for every sub area.
5) At this time, the histograms can be normalized.
6) Have all the histograms of sub areas connected in series, and then the features of the detected window are obtained.

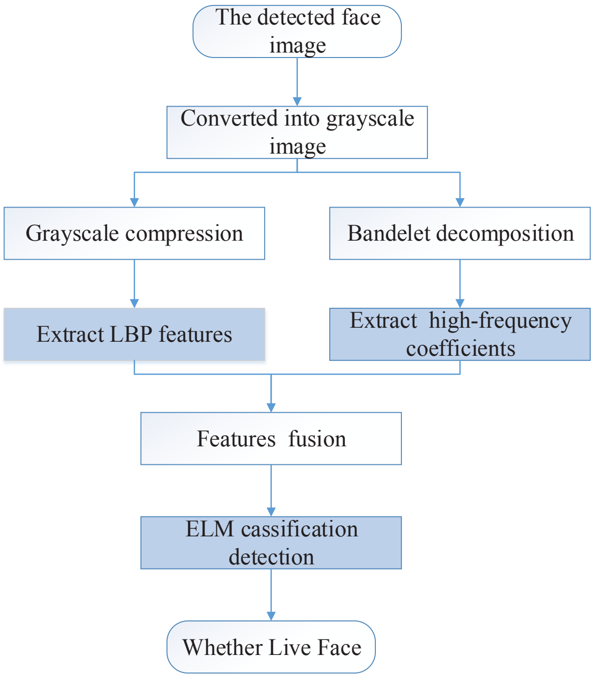

Figure IV. Flowchart of live face detection method based on LBP and Bandelet.

The process of getting statistical features of high-frequency coefficients in Bandelet transform is:
1) Input: grayscale image, quantization threshold T.
2) Conduct 2D wavelet transform on the image, orthogonal and biorthogonal wavelet transform can be used.
3) Establish quadtree segmentation for each sub band respectively, and get the best geometric flow directions of segmentation areas.
4) Conduct Bandelet transforms on each Bandelet area and get Bandelet coefficients.
5) Arrange Bandelet coefficients into matrix form according to a particular way.
6) Output: quadtree, the best geometric flow direction, Bandelet coefficients.

D. Extreme Learning Machine

We have conducted a statistical analysis and classification of the above two kinds of features. In this paper, basic ELM is adopted as the classifier. ELM, proposed by Guangbin Huang [24], is an algorithm to solve the single hidden layer neural networks. Under the condition of ensuring learning accuracy, the most obvious feature of ELM is to run faster than traditional learning algorithms for the traditional neural networks, especially for single-hidden layer feed forward neural networks (SLFN). ELM is a new type of fast learning algorithm, for the single-hidden layer neural network, and it can initialize the input weights and bias randomly to get the corresponded output weights.

For a single hidden layer neural network (as shown in Fig. 3), assume that there are N random samples (X_i, t_i), where $X_i = [x_{i,1}, x_{i,2}, \cdots, w_{i,n}]^T \in R^n, t_i = [t_{i1}, t_{i2}, \cdots, t_{im}]^T \in R^m$. n is the dimension of each feature vector X and m is the length of output vector t(m is 1 here because face detection is a binary classification problem, and t_i is 0 or 1).A single hidden layer

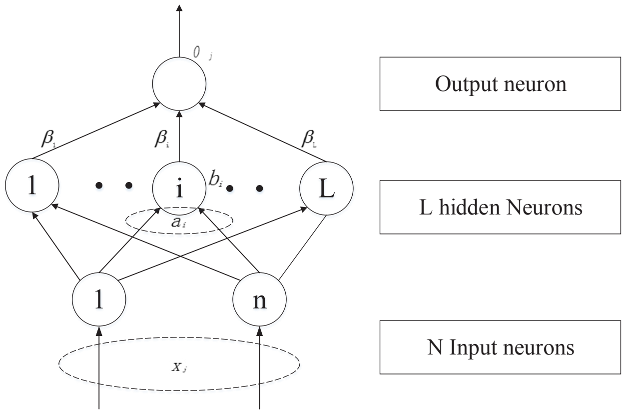

Figure V. SLFN: additive hidden nodes.

neural network with L hidden nodes can be expressed as:

$$\sum_{i=1}^{L} \beta_i g(W_i \bullet X_j + b_i) = O_j,\ j = 1, \cdots, N, \quad (1)$$

in this formulation, $f(x)$ is active function, $W_i = [w_{i,1}, w_{i,2}, \cdots, w_{i,n}]^T$ is the weight of the input, β_i is the weight of the output, b_i is the bias of the ith transient node. $W_i \bullet X_j$ represents the inner-product of W_i and X_j.

The target of Single layer neural network is to minimize the error of the output, which can be represented as

$$\sum_{j=1}^{N} \| o_j - t_j \| = 0 \ , \quad (2)$$

there are some β_i, W_i and b_i that are qualified for

$$\sum_{i=1}^{L} \beta_i g(W_i \bullet X_j + b_i) = t_j, j = 1, \cdots, N \ , \quad (3)$$

which can be represented by a matrix

$$H\beta = T \ , \quad (4)$$

where H is the output of the transient node, β is the weight of output, and T is the expected value of output.

$$H(W_1, \cdots, W_L, b_1, \cdots, b_L, X_1, \cdots, X_L) = \begin{bmatrix} g(W_1 \bullet X_1 + b_1) \cdots & g(W_L \bullet X_1 + b_L) \\ g(W_1 \bullet X_N + b_1) \cdots & g(W_L \bullet X_N + b_L) \end{bmatrix}_{n \times l}$$

$$\beta = \begin{bmatrix} \beta_1^T \\ \vdots \\ \beta_1^T \end{bmatrix}_{L \times m}, \quad T = \begin{bmatrix} T_1^T \\ \vdots \\ T_1^T \end{bmatrix}_{N \times m} \quad (5)$$

In order to train a single transient layer network, $\hat{W}_i, \hat{b}_i$ and $\hat{\beta}_i$

$$\| H(\hat{W}_i, \hat{b})\hat{\beta}_i - T \| = \min_{W,b,\beta} \| H((w_i, b)\beta) - T \| \quad (6)$$

where, $i = 1, \cdots, L$. The inference process above can be summarized as the following minimize loss function.

$$E = \sum_{j=1}^{N} (\sum_{i=0}^{L} \beta_i g((W_i \bullet X_j + b_i) - t_j))^2 \quad (7)$$

Some traditional algorithms based on gradient descent methods can be used to solve this problem, but the basic learning algorithm based on gradient needs to adjust all the parameters in the process of iteration. As opposed to this, in the ELM algorithm, once the input weights and hidden layer bias are randomly determined, the output matrix H of hidden layer is only determined. Training a single hidden layer neural network can be transformed into solving a linear system and the output weights can be determined.

IV. EXPERIMENTAL RESULTS

In order to test the algorithm's ability to identify live faces and fake faces, we use the public face database CASIA_FASD, print-attack and replay attack to test.

A. Print-attack Dataset

The print-attack dataset contains a short video of valid access and spoof attacks to 50 different identities. The spoof attack that is emphasized in this dataset is print attack only, whereby an impostor presents a printed photograph of the targeted identity in order to falsify the access to a face biometric authentication system. This dataset includes two different scenarios: (i) controlled background (the background is uniform) and (ii) adverse background (a non-uniform background). These scenarios provide a valid simulation of the attack environment. Table II shows the number of video in the print-attack dataset.

Table II. Number of videos in the print-attack dataset

Type	Train	Develop	Test	Total
Real-access	60	60	80	200
Phone-attack	90+90	90+90	120+120	200+200
Table-attack	240	240	320	800

B. Replay-Attack Dataset

The replay-attack dataset consists of 200 videos of valid access (with 375 frames each), and 1000 videos of attack attempts (with 240 frames each). As shown in Table III, the dataset is divided into three partitions, namely development, training and testing set. The development set is used for estimating the threshold value and training set is used for estimating any model parameters.

Table III Number of videos in the replay-attack dataset

Type	Train	Develop	Test	Total
Live	60	60	80	200
Print-attack	30+30	30+30	40+40	100+100
Phone-attack	60+60	60+60	80+80	200+200
Table-attack	60+60	60+60	80+80	200+200
Table-attack	360	360	480	1200

Each of these sets is generated by a video gallery of 15 clients for development and training, and 20 clients for testing. This means that the training and testing sets are disjoint and completely independent of each other.

C. CASIA-FASD dataset

Compared to other live face detection databases, CASIA-FASD database contains more abundant real face and fake face sample types. As shown in Table IV, there were a total of 50 people registered in the database. Each registered person corresponded to 12 face video sequences, including three real face videos and nine fake face videos. Three real face videos were collected by a low-quality USB webcam, a high-quality USB webcam and a webcam of model Sony NEX-5 respectively.

All the videos in the database were collected in an uncontrolled environment, and the background areas were complex and changeable. In order to fully consider different ways of attack, fake face sample types were more abundant in the database. First, high-resolution images of each target face were displayed on different media, including common A4 printing papers, glossy photo papers, and a high-resolution display frequency. After that, the face eye area printed on A4 papers was removed to simulate the blink attack method. The database was divided into training set and testing set, where the training set is composed of 240 video sequences from 20 targets and the test set is composed of 360 video sequences from other 30 targets. Take the rest samples which never participated in the training as the test set and the image numbers of train set and test set are shown in Tab. 1. We took the remaining samples, which never participated in the tarining, as the test set. The details of the test set and the training set are shown in Table IV.

Table IV Face images of train set and test set in CASIA database

Quality	Size	Train data			
		Liveness face	Spoof face		
			Bend	Cut	Video
high	640×480	20	20	20	20
medium	480×640	20	20	20	20
low	920×1080	20	20	20	20
Total		60	60	60	60
		Test data			
		Liveness face	Spoof face		
			Bend	cut	video
high	640×480	30	30	30	30
medium	480×640	30	30	30	30
low	920×1080	30	30	30	30
Total		90	90	90	90

In order to test the validity of the algorithm, this paper extracts LBP features of real and fake faces and wavelet features to classify and train ELM. Its detection accuracy is shown in Table V. This paper also adds the Bandelet features to LBP features and tests its detection accuracy for real and fake faces, as also shown in Table V.

From Table V, we can see that with the local binary pattern as the basic features, combined with Bandelet analysis, has an effect on the detection accuracy on CASIA dataset. It is noticed that using Bandelet analysis increases the feature dimension, which leads to improvement in the detection accuracy of the system significantly, from 93.87% to 97.97%; although the basic LBP features are easy to compute, its feature dimension 59 is greater than 12 under the analysis of LBP in comparison with Bandelet, which increases the system cost. The detection accuracy of LBP features which adds Bandelet analysis is 97.97%, and it is significantly greater than the detection accuracy of basic LBP features at 93.87%.

Table V. Comparison of LBP in combination with Bandelet features and other features

Samples	TP	TN	Detection accuracy	Feature dimensions
Basic LBP features	93.55%	94.06%	93.87%	59
Gray-level co-occurrence matrix	96.44%	91.13%	94.27%	8
All LBPV	91.84%	86.39%	88.03%	256
Uniform LBPV	88.13%	86.25%	86.95%	59
DoG (Curvature Driven Diffusions)			97.7%	512
LBP in combination with Bandelet	96.03%	95.88%	97.97%	12

Where TP denotes the detection accuracy of positive samples and TN denotes the detection accuracy of negative samples.

Compared with ALL LBPV and Uniform LBPV, LBP features under the analysis of Bandelet have obvious advantages. It reduces the feature dimensions and complexity of the algorithm, and at the same time it improves the detection accuracy. The detection accuracy of the proposed method declines, but the algorithm complexity reduces significantly compared with gray-level co-occurrence matrix and wavelet features. Therefore, reducing the algorithm complexity, while maintaining the detection accuracy, will be our future research focus.

Also, we compare the other method in Table V, Gray-level co-occurrence matrix and DOG methods has also been widely used in the extraction of image texture. Compared with the text algorithm, the size of DOG is too large and the computational complexity is large. Although the dimensions of co-occurrence gray matrix are small, the accuracy is not high.

Next, we compare the performance of LBP, Bandelet and Bandelet-LBP on three datasets. The images in Fig.8 show the ROC curves of Bandelet-LBP, LBP and Bandelet. The performance of proposed algorithm is better than the base LBP and Bandelet on three dataset. Figure VIa shows the overall performance when trained and tested on CASIA dataset. Figure VIb shows the overall performance when trained and tested on print-attack dataset. Figure VIc shows the performance on replay-attack dataset. In these three datasets, the Bandelet-LBP features perform the best, and our method is more robust on three datasets than LBP and Bandelet features.

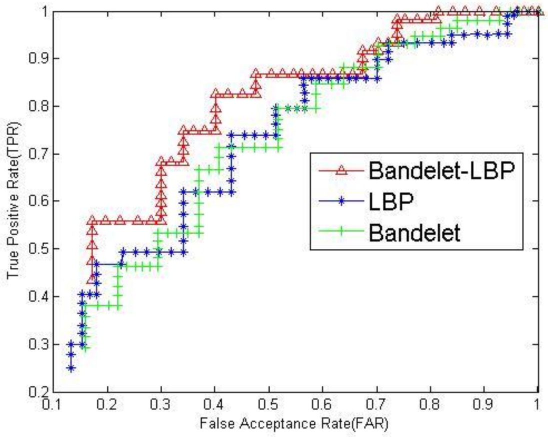

(a)

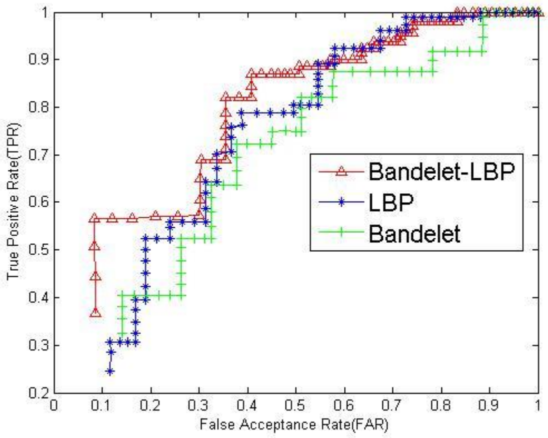

(b)

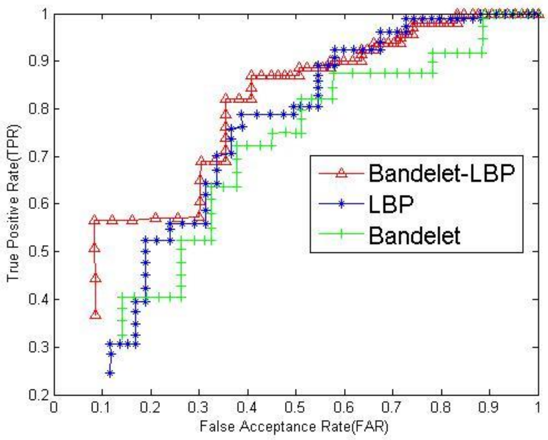

(c)

Figure VI Comparison of ROC curves of different algorithm on three datasets. (a) print-attack dataset (b) CASIA dataset (c) replay-attack dataset.

V. CONCLUSION

This paper proposed a live face detection method based on Bandelet analysis under the analysis of texture feature differences among live faces, photo faces, and video faces. This method conducts a Bandelet analysis on grayscale images of faces and extracts local binary pattern features based on the Bandelet analysis. The feature of the image is obtained by divided into 100 blocks and set the weight value, which can enhance the important characteristics of the image and reduce the noise impact. Finally, the characteristics of the two algorithms are fused, and the learning and classification are entered into ELM. Experimental results show that the algorithm can reduce the computational complexity and improve the detection accuracy. But in practical applications, there are many interference factors to be considered, such as the influence of illumination condition and high-resolution cameras which are used to shoot face photos and videos. This will be in the focus of our future research.

REFERENCES

[1] Z. Boulkenafet, J. Komulainen, A. Hadid, "Face Spoofing Detection Using Colour Texture Analysis", IEEE Transactions on Information Forensics and Security,2016, pp. 1818-1830.

[2] W. Kim, S. Suh, J. Han, "Face Liveness Detection From a Single Image via Diffusion Speed Model" IEEE Transaction on Image Processing, 2015, pp. 2456-246.

[3] D.F. Smith, A. William, B.C. Lovell. Face Recognition on Consumer Devices: Reflections on Replay Attacks. Information Forensics and Security IEEE Transaction on. 2015, pp. 736-745.

[4] N. Erdogmus, S. Marcel, Spoofing Face Recognition With 3D Masks. IEEE transactions on information forensics and security, 2014, pp 1084-1097.

[5] D. Gong, Z. Li, W.L. Huang, X.L. Li, D. Tao. Heterogeneous Face Recognition: A Common Encoding Feature Discriminant Approach. IEEE Transaction on circuits and system for video technology. 2017. pp. 2079-2089.

[6] I. Kim, J. Ahn, D. Kim, Face Spoofing Detection with Highlight Removal Effect and Distortions. IEEE International Conference on Systems. 2016. pp. 1-6.

[7] D. Wen, H. Han, A.K. Jain. Face Spoof Detection With Image Distortion Analysis. IEEE Transaction on forensics and security. 2015.pp. 746-761.

[8] M. Uzair, A. Mahmood, A. Mian. Hyperspectral Face Recognition With Spatiospectral Information Fusion and PLS Regression. IEEE Transactions on image processing. 2015. pp. 1127-1137.

[9] J. Galbally, S. Marcel, J. Fierrez, Image Quality Assessment for Fake Biometric Detection: Application to Iris, Fingerprint and Face Recognition, IEEE Transactions on Image Processing, 23 (2014) 710-724.

[10] S. Karungaru, M. Fukumi, N. Akamatsu. Face recognition in colour images using neural networks and genetic algorithms. International Journal of Computational Intelligence and Applications, 2005, pp 55-67.

[11] S.R. Arashloo, J. Kittler, W. Christmas, Face Spoofing Detection Based on Multiple Descriptor Fusion Using Multiscale Dynamic Binarized Statistical Image Features, IEEE Transaction on information and security, 2015, pp. 2396-2407.

[12] G. Pan, L. Sun, Z. Wu, S. Lao, Eyeblink-based Anti-Spoofing in Face Recognition from a Generic Web camera, in IEEE International Conference on Computer Vision, 2007, pp. 1-8.

[13] Santosh T, Norman P, David W, et al. Detection of Face Spoofing Using Visual Dynamics. IEEE Transaction on Information Forensics and Security. 2015. pp. 762-777.

[14] W. Yin, Y. Ming, L. Tian. A face anti-spoofing method based on the optical flow field. 2016 IEEE 13th International Conference on Signal Processing (ICSP). 2016. pp. 1333-1337.

[15] A. Pinto, H. Pedrini, W.R. Schwartz, A. Rocha, Face Spoofing Detection Through Visual Codebooks of Spectral Temporal Cubes. 2015. pp. 4726-4740.

[16] W. Paier, M. Kettern, A. Hilsmann, P. Eisert, A Hybrid Approach for Facial Performance Analysis and Editing. IEEE Transaction on circuits and system for video technology. 2017. pp. 784-797.

[17] Z. Yu, G. Michael, B. Chris, C. Jun, X. Yong. Hybrid hierarchical clustering-piecewise aggregate approximation, with applications. International Journal of Computational Intelligence and Applications. 2016. p 165019(26 pp).
[18] N. Werghi, C. Tortorici, S. Berretti, A. D. Bimbo. Boosting 3D LBP-Based Face Recognition by Fusing Shape and Texture Descriptors on the Mesh. 2016. pp. 964-979.
[19] K. Patel, H. Han, A.K. Jain, Secure Face Unlock: Spoof Detection on Smartphones. IEEE Transaction on information and security. 2016. pp. 2268-2283.
[20] T.D.F. Pereira, J. Komulainen, A. Anjos, J.M.D. Martino, A. Hadid, M. Pietikäinen, S. Marcel, Face liveness detection using dynamic texture, Eurasip Journal on Image & Video Processing, 2014 (2014) 1-15.
[21] T. Edmunds, A. Caplier, Fake Face Detection Based on Radiometric Distortions. IEEE Conference Publications. 2016, pp, 1-6.
[22] Z. Akhtar, C. Micheloni and G. L. Foresti, "Biometric Liveness Detection: Challenges and Research Opportunities," in IEEE Security & Privacy, vol. 13, no. 5, pp. 63-72, Sept.-Oct. 2015.
[23] A. Lutz, K. Grace; N. Messer. Bandelet transformation based image registration. 2015 IEEE Applied Imagery Pattern Recognition Workshop (AIPR). 2015. pp. 1-6.
[24] L.L.C. Kasun, H. Zhou, G.B. Huang, and C.M.Vong, “Representational Learning with Extreme Learning Machine for Big Data”, IEEE Intelligent Systems, 2013, pp. 31-34.

Haiqing LIU, acquired engineering PHD degree in Computer Application Technology from Wuhan University on December 2001. She went to WPI (Worcester Polytechnics Institute) in USA as a visiting scholar for 1 year since April 2004. She was employed as an associate professor and master’s supervisor by Wuhan University since October 2002, and transferred to Control and Computer Engineering Academy in NCEPU (North China Electric Power University) later in May 2005. She has been engaged in research and development work related to Software Engineering, Database and Artificial Intelligence since 1988.

Shuhua HAO, master degree candidate in North China Electric Power University, Beijing, China. Her research interests include power system and spooling face recognition.

Yuancheng Li, received the Ph.D. degree from University of Science and Technology of China, Hefei, China, in 2003. From 2004 to 2005, he was a postdoctoral research fellow in the Digital Media Lab, Beihang University, Beijing, China. Since 2005, he has been with the North China Electric Power University, where he is a professor and the Dean of the Institute of Smart Grid and Information Security. From 2009 to 2010, he was a postdoctoral research fellow in the Cyber Security Lab, college of information science and technology of Pennsylvania State University, Pennsylvania, USA.

Extension of RFID Based Indoor Localization Systems With Smart Tags

Tamás Helfenbein, Roland Király, Márton Töröcsik, Emil Tóth and Sándor Király

***Abstract*—The indoor localization problem is a method of identifying and finding position (co-ordinates) of requested objects in a well defined area of interest (AoI) in buildings. Beside identification, localization is an important task in several complex industrial environments. Assigning unique Radio Frequency IDentifier (RFID) tags to the objects both the identification and the localization problem can be solved.**

In this paper, RFID based indoor localization systems, methods, and protocols are analysed. A novel Smart Tag platform called Blackforest with integrated self localization capabilities is introduced. This device can be in either transmitter or receiver role to ensure fast prototyping of localization environments. Higher temporal positioning possibilities and sensor fusion techniques are introduced using the BlackForest nodes. The radiofrequency (RF) characteristcs of the device were analyzed and a localization system was built using Blackforrest nodes. The localization architecture, methods and system configurations are described. After calibration, the suitable accuracy of RFID indoor localization using BlackForest Smart Tags is proven in an indoor office scenario.

A hierarchical localization protocol stack is introduced in order to extend existing indoor RFID localization systems using intelligent and co-operative antenna systems with novel SmartTags.

***Index Terms*—Indoor localization, Self Localization, Smart Tag, RFID**

I. Introduction

Radio Frequency IDentification (RFID) is an advanced and emerging technology to identify objects based on radio frequency signal transmission and/or reception. Therefore, RFID systems are frequently used to help information systems manage objects in difficult and/or large environments. Besides identification of the tagged object, determining the location is one of the most important and also the most challenging tasks. RFID systems typically consist of readers with antennas and RFID transponders. The reader-antenna pairs and the tags can be fixed (deployed) or mobile. We are focusing on systems that have an infrastructure consisting of fixed reader-antenna pairs and mobile tags on the objects that need to be localized. Mobile readers are not excluded from the system, but are not necessarily parts of the infrastructure. In our research, three types of system architectures can be distinguished, namely Smart Reader Network (SRN), Smart Tag (ST) and Hybrid architectures.

The SRN architecture consists of intelligent reader-antenna pairs connected to a network or a computer server and inexpensive (e.g. passive UHF RFID) tags. In this system architecture, localization is made by the intelligent infrastructure (ambient intelligence) and location information is generated on the infrastructure side. In the ST system, intelligent, active RFID tags are used with (almost) traditional reader-antenna pairs. In this case, self-localization has to be done by the tag and the (self) location information is generated on the tag side. In the hybrid solution, concept SRN and ST are combined.

In conclusion, the article details our practical results in RFID based localization solutions. The prototype of a new generation of Smart Transponder is described in Section III, that is capable of self-localization based on information obtained from RFID antennas. Our ideas on hybrid applications and the combination of RFID systems with other technologies are also detailed. The self-localizing transponder and theconnected middleware resting on mathematical foundations can be used with significantly greater precision for indoor localization than current devices.

In the following section, we analyse the RFID based localization methods, systems and our previous works in Section II. Introducing the novel self localization concept is followed by the description of hardware prototype of Smart Tag called BlackForest and localization methods in Section III. The results and measurements are demonstrated in office environments in Section IV.

Localization methods are based on principles, models, measurements, and evaluation methods. A principle is a plan that determines what parameters to model, measure, and evaluate. [1][2] In case of multilateration (or trilateration) we have to determine distances using measurements and models, thus the position can be estimated from the best candidates for intersection of spheres or circles. In case of triangulation we have to determine angles and estimate position using the best candidates for intersection of directions given by the angles. We can also calculate position from distance differences using the best candidates for intersection of paraboloids.

Modelling is an important part of a localization system. Based on the principle, the environment and the given hardware devices we can assume different types of antenna models,

T. Helfenbein is with Research Lab, Chebio Ltd., e-mail: tamas.helfenbein@chebio.net

R. Király is with Institute of Mathemathics and Informatics, Eszterházy Károly University of Applied Sciences, e-mail: kiraly.roland@uni-eszterhazy.hu

M. Töröcsik is with the Institute for Infocommunication Technologies, Bay Zoltán Nonprofit Ltd. For Applied Research, e-mail: marton.torocsik@bayzoltan.hu

E. Tóth is with the Institute for Infocommunication Technologies, Bay Zoltán Nonprofit Ltd. For Applied Research, e-mail: emil.toth@bayzoltan.hu

S. Király is with the Institute of Mathemathics and Informatics, Eszterházy Károly University of Applied Sciences, e-mail: kiraly.sandor@uni-eszterhazy.hu

The RFID research project was supported by the European Union and the State of Hungary, co-financed by the European Social Fund in the framework of TÁMOP-4.2.2.C-11/1/KONV-2012-0014.

propagation models, kinematic models, and error models that can be used to refine measurements and create perception from the measured data. The result of the measurement is the input of our models; thus, the measured parameters must be determined using the models and the selected principle.

Using triangulation we can measure the phase difference of arrival (PoA), angle of arrival[1] (AoA), or the angle of departure[2] (AoD). Using multilateration we can measure the time of arrival[3] (ToA) or the received signal strength (RSS). In the case of distance difference, we can measure the time difference of arrival[4](TDoA).

Evaluation is typically an optimisation using the measured data and given models. Fingerprinting is a widely used method for evaluation that means we have to measure signal parameters offline at different locations. Using the measured signal parameters we can infer to the best candidate from (or between) the recorded points.

II. Related works

The ”You are here” (YAH) map is a basic type of localization system. Using acoustic, visual, or radio-frequency (RF) landmarks one can determine its location close to the landmark. It can be used by humans or machines. The landmarks can be QR codes or - in our case - NFC tags for instance. Fingerprinting based on a received signal strength indicator (RSSI) is often used for RFID localization [3] together with different types of classification and machine learning methods [4][5].

Models based on RSSI and Probabilistic Localization Algorithm (PLA) are also used together [6]. Propagation and path loss are modelled, and using the probabilistic distribution of the RSSI, location can be estimated by a Bayesian localization scheme. Data analysis methods like multidimensional scaling (MDS) can be used to locate active RFID tags based on RSS measurements [7]. Phase difference (PoA) estimation using multiple antennas is often used to locate RFID tags [8][9]. PoA can be augmented with other methods. At the reader side, reference tags and different reader output power setting strategies can be used to locate a tag. [10][11]

RFID tags can be modified or extended with other technologies to achieve the best results. Hybrid systems use acoustic [12], visual [13][14], or inertial sensor data [15]. Simultaneous Localization and Mapping (SLAM) methods can be used to determine the location of mobile readers and RFID tags. Typically, additional geometric information is needed [16]. A modified tag called ”sense-a-tag” can measure backscattering in the near field and save this kind of location information [17]. Using an RFID reader and normal RFID tags placed on known locations, the system can track ”sense-a-tags” attached to the objects.

In our previous work, a novel antenna design and a localization concept were defined [19]. The novel device was called an “Nodding antenna”, that can change its characteristics and ”look” to 6 directions in space with different output power. Using this, the RFID localization can be extended beyond the area covered by the RFID reader system. The novel concept called Location on Tag (LoT) is a Smart Reader Network (SRN) based localization protocol that uses the limited memory of the passive RFID transponder to store location information. The Smart Readers can determine the position of the tag and then write this current position into a circular list defined in the tag memory. The path of the tags which are travelling with this information can be reconstructed by other Smart Readers. A mathematical framework was developed to recover the possible path of moving RFID transponders in indoor environments [20][21]. This framework is suitable in cases when the tag becomes unreadable or enters into an uncovered area.

III. Self localization methods and the hardware prototype

The Smart Tag (ST) RFID localization architecture is the inside out version of the SRN solution. In this case, tag self-localization is done onboard using an almost typical reader infrastructure to estimate the own position of the tag in a reference coordinate system.

The components of this ST system can be seen in Figure 1. The system consists of multiple readers/transmitters with known positions and IDs. These reader parameters should be transmitted to the Smart Tag. Using distance and/or angle estimations, Smart Tag can determine its position (using trilateration, triangulation or probability based methods). In the following sections we describe the requirements of components, measurements, methods, and the hardware/software components of the Smart Tag localization system architecture.

To calculate the position the Smart Tag has to measure distances or angles. We decided to measure the signal strength indicator (RSSI) of the readers in real time. This can lead to distance estimation or angle calculation (in the case of object rotating). The reader-antenna pairs have to be distinguished; therefore, the reader-antennas are broadcasting unique ID-s. Methods require the coordinates of the antennas for position estimation; thus, the antenna ID-Coordinate pairs should be transmitted to the tag memory. Smart Tags have to execute complex algorithms onboard, thus one needs enough memory and computational capacity. Active (or semipassive) ones have to be used, since an external power supply of the tag is needed.

The input signal for RSS based localization is suffering from artifacts caused by filtering that is typically made by the consumer RF receiver circuit/device to filter out dynamic changes to produce more stable (and repeatable) RSS values. A method that uses propagation models can take advantage of the low level (raw) RSS signal but cannot deal with a signal that is filtered and has low temporal resolution. Moreover, we

[1]Angle of arrival (AoA) measurement is a method for determining the direction of propagation of a radio-frequency wave incident on an antenna array. AoA determines the direction by measuring the Time Difference of Arrival (TDoA) at individual elements of the array.

[2]Angle of Departure measurement is done when the transmitter transmits through multiple antennas and the receiver resolves the angle of signal departure based on the received signals.

[3]ToA the travel time of a radio signal from a single transmitter to a remote single receiver.

[4]TDoA is the time differences between received signals measured with multiple antennas. Each measurement defines a hyperboloid of possible locations of the transmitter.

designed a universal device to measure RSS values directly in our experiments. The device called BlackForest can monitor RF channels from an SMA[5] antenna connector in real time from 100MHz to 1GHz with 1Hz resolution and mix it down to a 200-40000Hz baseband. The I and Q signal can be processed by analog-digital converters (ADs) of an audio card since I and Q signals are available on a 3.5mm stereo audio jack connector. The received sensitivity is adjustable from 0 to 60 dB and the modulation method is also selectable from the list of ASK[6], OOK[7], BPSK[8], FM[9] and FSK[10]. For further experiments and localization method evaluation, the BlackForest device has a 3D gyroscope and an accelerometer.

To have a complete system, BlackForest can also transmit (Rx and Tx adjustable with jumper), and the transmission frequency is also adjustable. The panel is supplied by external 5V, the other components are supplied via LDO[11] modules with 3.3V and 2.4V regulated outputs.

The transmission and the received functionality make BlackForest a universal platform to evaluate experimental localization methods without a large amount of deployable, fixed RFID reader-antenna pairs. Furthermore, it is possible to analyse different situations, system configurations, and scales. In a current setup, the readers are BlackForest-Tx nodes and the node that is being localized is a BlackForest-Rx node and it is connected to a sound card in a PC. The transmission frequency is in the 868 MHz band, the frequency of channel n is $868MHz + n * 1KHz$. We identify reader nodes using frequency division multiplexing (FDM), which means that each reader transmits signals at different frequencies. The received signal strength at a given reader frequency means a distance candidate with error factors such as path attenuation. Localization methods can take into account these error factors using propagation models and/or mapping. Using the BlackForest hardware, our goal is to analyze the applicability of different propagation models for RFID localization solutions in different environments.

The arrangement of the infrastructure is also an important part of our research, therefore we were considering different optimization methods to find optimal positions of the readers (beacons) in a given environment. To ensure a higher spatial and temporal quality of RFID localization, transponders have to be extended with sensors that can measure relative displacement and rotation of the tag between RF localization measurements or in areas that are not covered by readers.

[5]SMA (SubMiniature version A) connectors are semi-precision coaxial RF connectors.

[6]Amplitude-Shift Keying is a form of amplitude modulation that represents digital data as variations in the amplitude of a carrier wave.

[7]On-Off Keying denotes the simplest form of Amplitude-Shift Keying (ASK) modulation that represents digital data at the presence or absence of a carrier wave.

[8]Binary Phase-Shift Keying is the simplest variant of Phase-Shift Keying and conveys data by switching the phase of a reference signal.

[9]Frequency Modulation is the encoding of information in a carrier wave by varying the instantaneous frequency of the wave.

[10]Frequency-Shift Keying is a frequency modulation scheme in which digital information is transmitted through discrete frequency changes of a carrier signal

[11]A low-dropout or LDO regulator is a DC linear voltage regulator that can regulate the output voltage even when the supply voltage is very close to the output voltage.

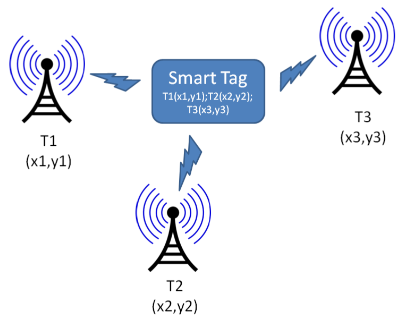

Fig. 1. BlackForest Smart Tag localization arrangement

Inertial sensors like the accelerometer and gyroscope can help to increase the temporal resolution of the localization. Therefore, we designed BlackForest to be able to measure 3 axes of acceleration and angular velocity using an accelerometer and a gyroscope IC. After choosing the sensors, we considered high level sensor fusion methods to increase the quality of the RF localization using the inertial measurements.

The basic BlackForest positioning system (Figure 1) consists of at least 3 BlackForest as transmitters: $T1, T2, T3$ and at least one BlackForest Smart Tag as an active receiver: $SmartTag$. The transmitters $T1, T2, T3$ are configured as RFID transmitters (Tx nodes) and the receiver $SmartTag$ is configured as a receiver node (Rx node). Transmitters are arranged in a nodes of a triangle on a plane, thus, the positioning area is the area covered by at least 3 transmitters. This can be seen in Figure 2.

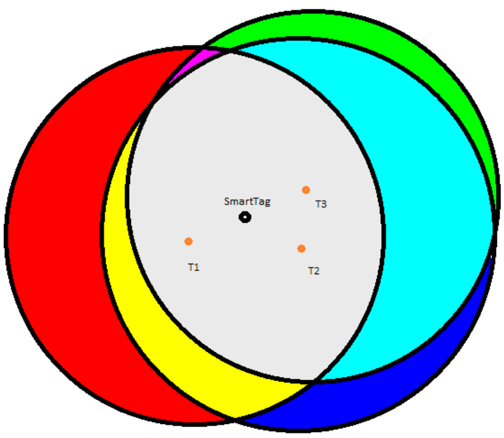

Fig. 2. BlackForest transmitter coverages

To locate the BlackForest SmartTag, we use a log distance path loss model (LDPL). This expresses a relationship between the received signal strength (RSS) and the distance from the transmitter [22].

$$P_{rx} = P_{tx} - P_{ref} - 10\alpha \log d - X\sigma \quad (1)$$

Here, P_{rx} is the power of received signal (RSS), P_{tx} is the transmitter output power, P_{ref} is the received signal power at the reference distance $(1m)$, d is the unknown distance from the transmitter to the receiver node, α is an exponential model parameter and X is the term for further attenuation. The measurements can be done in multiple coordinates at different distances from the transmitters.

From these measurements, the model parameters (α,X) can be estimated by using a nonlinear fitting method. In this case, the Levenberg–Marquardt algorithm[12] was chosen to calculate the parameters of the LDPL models. Transmitters can broadcast their positions, IDs and the calibrated attenuation parameters, thus, these parameters are downloaded to the tag.

For a transmitter, the distance can be estimated using the following formula:

$$d = 10^{\frac{-P_{rx}-P_{offset}}{10\alpha}} \tag{2}$$

where $P_{offset} = P_{tx} - P_{ref}$.

Once LDPL models are calibrated properly, the transmitter can estimate the position by building a possibility map from the measured values and transmitter coordinates and LDPL parameters.

The transmitters are communicating their IDs (Ti), coordinates(xi, yi) and model parameters (Pi), therefore, when the $SmartTag$ arrives into the positioning area it registers these values into its memory:

$$\begin{aligned} D =&\{(T1, P1, x1, y1),\\ &(T2, P2, x2, y2), (T3, P3, x3, y3)\} \end{aligned} \tag{3}$$

BlackForest receiver node $SmartTag$ measures RSS values for each visible Ti transmitters and registers them with the transmitter coordinates as measurements:

$$\begin{aligned} M =&\{(M1, P1, x1, y1),\\ &(M2, P2, x2, y2), (M3, P3, x3, y3)\} \end{aligned} \tag{4}$$

Possibility map onboard estimation is a hard task for embedded systems, therefore, the calculation is done in an equidistant grid of NxM points over the positioning area. Possibilities from an individual distance measurement based on the LDPL model is represented as a Gaussian along a circle with the empiricaly set $\sigma = 2.5m$ parameter. The maximum possibility value can be chosen as $SmartTag$ position candidate.

The transmitters are broadcasting multiple LDPL model parameters depending on the context. This is formed in the attenuation parameter X. Typically, the parameters can be determined for each rooms in the building to model the attenuation of the walls between the transmitter and the SmartTag node. Since the tag can test multiple configurations of the model parameters (depending on the room) for a measurement set , the best candidate with the highest possibility can be chosen.

Previous position and inertial sensor measurements over time was used both as selectors for Area of Interest (AoI) and by filtering the current probablity map. A 2D Gaussian filter[13] with $\sigma = 2m$ was chosen and was used at the point that was estimated from of the previous locations and intertial sensor measurements using an Extended Kalman Filter (EKF)[14] [23].

An extended version of the BlackForest node (EBF) was developed with a 2D linear square array of 4 antennas. The array is capable of Angle of Arrival (AoA) measurements. The estimation of the angles was done using the ESPRIT method [24][25]. Alternatively, the position with lower accuracy can be calculated from these directions only, using the non-linear optimization proposed in [26]. Although we used the directions from the AoA measurements to futher filter the probability map using multiple one-dimensional Gaussian filters with the empirically set $\sigma = 1.5m$ parameter along the given direction.

The novel tag can be used in the previously developed RFID localization system: Location on Tag (LoT) concept [19] was easily adapted to the system since the location is determined at the tag side.

To enhance the possibility of finding the location of the tag, all of the methods can be integrated in one system. Smart Tag can determine and store its location and this data can be sent to the readers. In this case, the reader can determine the validity of the location of the Smart Tag. If it fails, the following methods are performed.

In case of the Smart Reader localization method using LoT [19], the locations (path) are in the tag memory. Smart Readers execute the defined LoT algorithms to determine the path of the tag if the tag is in the covered area. If it is known that the tag is in the area but it cannot be read for a while (e.g. because it is temporarily in an uncovered area), its position can still be estimated using the mathematical framework (see in [20], [21]). Using these three methods, location can be determined or estimated in all cases and by a discrete time. This combination of localization methods is suitable for various indoor and outdoor localization tasks.

IV. RESULTS

BlackForrest receiver node measures RSS values utilizing $868MHz$ frequency and $-15dBm$ output power at the transmitter node. An Anritsu MT8222A BTS Master device was placed at different distances from the transmitter node. The results can be seen in Figure 4.

On the second floor of a typical office building (including walls) a room measuring 40m x 30m was chosen as the localization area. Positioning measurements using the LDPL model was started with the model calibration process (Figure 3). We measured RSS for different distances from the transmitter and fitted a model using the Levenberg–Marquardt algorithm (LMA).

We used 3 BlackForest nodes as transmitters and one BlackForest SmartTag receiver node at the position $X = 138$ and $Y = 170$. This arrangement is shown in Figure 5.

The framework can calculate the possibility of the tag position in a co-ordinate. This can be visualized for a set of measurement as a probability map. A calculated possibility map is shown in Figure 6. The maximum possibility is at the

[12]The Levenberg–Marquardt algorithm is used to solve non-linear least squares problems. These minimization problems arise especially in least squares curve fitting.

[13]Gaussian filter is a filter whose impulse response is a Gaussian function (or an approximation to it).

[14]Kalman filtering is an algorithm that uses a series of measurements observed over time, containing statistical noise and other inaccuracies, and produces estimates of unknown variables.

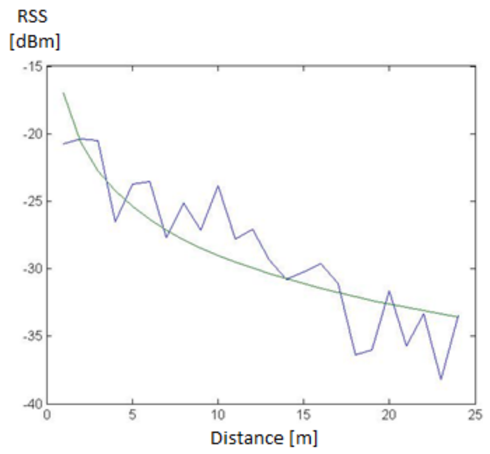

Fig. 3. Measured RSS values at different distances (blue) used for calibration and the fitted model (green)

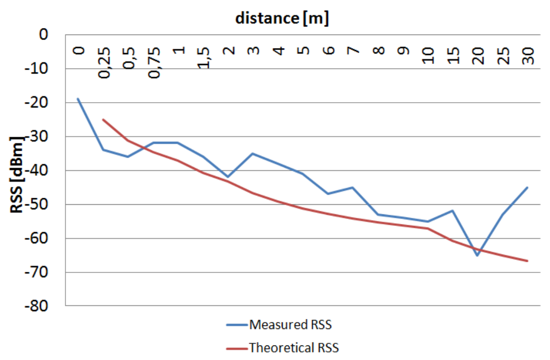

Fig. 4. Measured and theoretical RSS values

coordinates $X = 116$ and $Y = 144$. For this measurement, RSS based the localization error is $3,41m$.

After the previous location based and DoA filtering process, estimation ended in $X = 130$ and $Y = 166$, thus, the overall localization error is $0.89m$. These results can be seen in Figure 7 and 8.

After single measurements, multiple measurements were done and also multiple nodes were placed in the positioning area. We measured 20 samples at different locations. We used 2, 5 and 10 receiver nodes to analyze the effect of the multinode environment to the positioning accuracy. We found that the accuracy did not suffer of additional errors due to the increase of the number of the SmartTags. The average results can be seen on Table I.

TABLE I
POSITIONING ERROR IN MULTINODE ENVIRONMENT

Number of SmartTags	Average positioning error
1	0.92m
2	0.76m
5	0.87m
10	0.94m

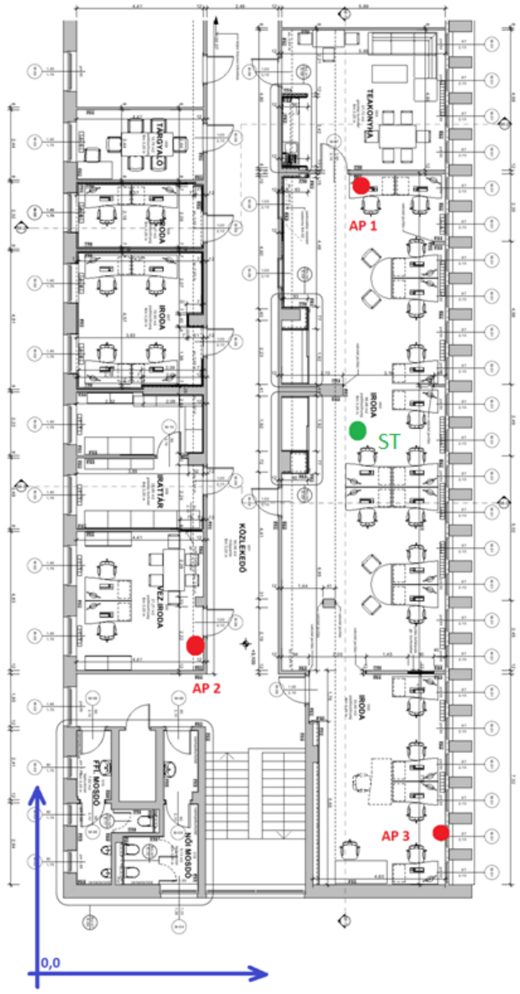

Fig. 5. System arrangement: reference coordinate system (blue), Smart Tag (green), transmitter nodes (red)

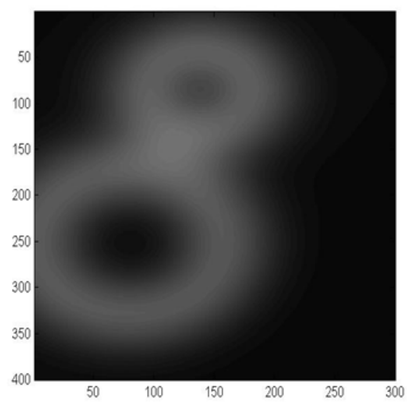

Fig. 6. Possibility map in the resolution of 10 cm

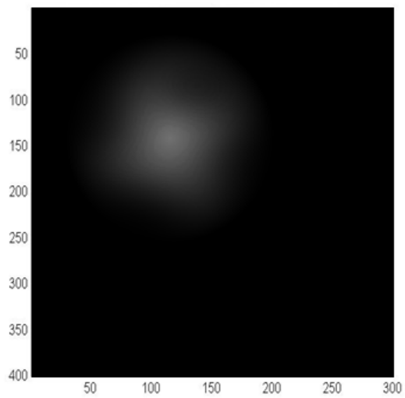

Fig. 7. Possibility map filtered by the previous location information in the resolution of 10 cm

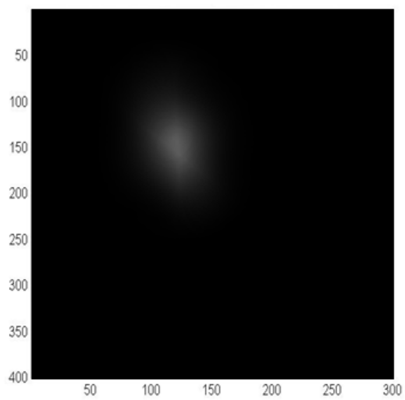

Fig. 8. Possibility map filtered by the previous location information and DoA, in the resolution of 10 cm

Table II summarizes our results compared to some of the recent and available RFID based positioning solutions.

TABLE II
Positioning error comparison

System	Average positioning error
VLSL and LANDMARC[27]	2.1m
BlackFIR[28]	1.0m
Our method	0.8m

However, our method requires calibration of the used models and uses signal processing at the tag side, it does not require complex antennas at the system side, thus, the infrastructure is cost effective.

V. Conclusion

After discussing systems and methods for RFID based indoor positioning, a novel SmartTag platform called Blackforest and an improved version called EBF were introduced. Later is capable of measuring RSS, Angle of Arrival (AoA) and inertial motion parameters. A novel method based on the system of EBF SmartTags and multiple transmitters was presented for self localization. The method uses RSS based adaptive LDPL models and Kalman filtering for position estimation and AoA measurements for position refinement. The novel device platform and localization method was tested in indoor office scenario and it was found as a solution in terms of mean positioning error against other available methods. Moreover, the system can efficiently extend previous localization architectures.

To enhance the possibility of finding the location of the tag, the self-localization, the Location-on-Tag method and the mathematical framework can be integrated in one system as a hierarchical localization architecture. This combination of localization methods is suitable for various indoor and outdoor localization tasks.

As a future research project, we would like to design and analyse a new, smaller version of the SmartTag prototype and introduce enhanced adaptive distance models and localization methods to the indoor positioning platform.

Acknowledgment

The authors would like to thank to the members of BAY-IKTI, namely Márton Törőcsik, Emil Tóth, Péter Pók, Gábor Kis-Vámosi, Ádám Ács and the members of Institute of Mathematics and Informatics, EKE.

The authors and institutes also would like to thank the support of European Union and the State of Hungary, and the European Social Fund.

References

[1] Mathieu Bouet, Aldri L. dos Santos, *RFID Tags: Positioning Principles and Localization Techniques*, Wireless Days, 2008.
[2] Christian Núñez Álvarez, Cristian Crespo Cintas, *Accuracy evaluation of probabilistic location methods in UWB-RFID systems*, Master Thesis, 2010.
[3] Shyam Sundar Prasad, Chanakya Kumar, *Comparison between Innovative Approaches of RFID Based Localization Using Fingerprinting Techniques for Outdoor and Indoor Environments*, International Journal of Soft Computing and Engineering (IJSCE), 2013.
[4] Jiaqing Wu, *Three-Dimensional Indoor RFID Localization System*, PhD Dissertation, 2012.
[5] Siddika Parlak, Ivan Marsic, *Non-intrusive Localization of Passive RFID Tagged Objects in an Indoor Workplace*, IEEE International Conference on RFID-Technologies and Applications, 2011.
[6] Wenbo Shi and Vincent W.S. Wong, *MDS-based Localization Algorithm for RFID Systems*, IEEE International Conference on Communications (ICC), 2011.
[7] Long Xiao, Ye Yin, Xiangnong Wu, Jianwei Wang, *A Large-scale RF-based Indoor Localization System Using Low-complexity Gaussian Filter and Improved Bayesian Inference*, RADIOENGINEERING, 2013.
[8] Cory Hekimian-Williams, Brandon Grant, Xiuwen Liu, Zhenghao Zhang, and Piyush Kumar, *Accurate Localization of RFID Tags Using Phase Difference*, IEEE RFID, 2010.
[9] Yimin Zhang, Moeness G. Amin, and Shashank Kaushik, *Localization and Tracking of Passive RFID Tags Based on Direction Estimation*, International Journal of Antennas and Propagation, 2007.
[10] Kirti Chawla, Gabriel Robins, Liuyi Zhang, *Object Localization Using RFID*, ISWPC'10 Proceedings of the 5th IEEE international conference on Wireless pervasive computing, 2010.
[11] Kirti Chawla, *An RFID-Based Object Localization Framework and System*, PhD Dissertation, 2014.
[12] Yi Zhao, Joshua R. Smith, *A battery-free RFID-based indoor acoustic localization platform*, IEEE International Conference on RFID, 2013.

[13] Songmin Jia, Jinbuo Sheng and Kunikatsu Takase, *Development of Localization Method of Mobile Robot with RFID Technology and Stereo Vision*, Computer Vision, ISBN 978-953-7619-21-3, 2008.

[14] Younes Raoui, El Houssine Bouyakhf, Michel Devy, Fakhita Regragui, *Metrical Mapping and Self Localization with RFID Technology and Visual Landmarks*, Applied Mathematical Sciences, Vol. 5, 2011.

[15] Alessio Levratti, Matteo Bonaiuti, Cristian Secchi, Cesare Fantuzzi, *An Inertial/RFID Based Localization Method for Autonomous Lawnmowers*, 10th IFAC Symposium on Robot Control, 2012.

[16] Dirk Hähnel, Wolfram Burgard, Dieter Fox, Ken Fishkin, Matthai Philipose, *Mapping and Localization with RFID Technology*, ICRA '04. 2004 IEEE International Conference on Robotics and Automation, 2004.

[17] Akshay Athalye, Vladimir Savic, Miodrag Bolic, Petar M. Djuric, *Novel Semi-Passive RFID System for Indoor Localization*, IEEE Sensors Journal, 2013.

[18] Intelliflex On-Demand Data Visibilty - Intelliflex Readers, http://www.intelleflex.com/Products.asp

[19] Roland Király, Tamás Helfenbein, Sándor Király, Emőd Kovács and Tamás Balla, *Novel concepts and devices in RFID based indoor localization using Smart Reader Networks and Intelligent Antennas*, Infocommunications Journal, Volume IX. Number 2., 2017.

[20] Zoltán Ruzsab, Zsolt Parisekb, Roland Király, Tibor Tómács, Tamás Szakács, Henrik Hajagos, *Build a mathematic based RFID localization framework*, Annales Mathematicas et Informaticae 44 (2015), selected papers Selected papers of the 9th International Conference on Applied Informatics ISSN 1787-5021 (Print) ISSN 1787-6117 (Online) 165-176

[21] Szakács Tamás, Ruzsa Zoltán, Király Roland, Parisek Zsolt, *Mathematics-based localizaion framework*, Networkshop 2014, ISBN: 978-963-88335-5-6, 2014.

[22] Scott Y. Seidel, Theodore S. Rappaport, *914 MHz Path Loss Prediction Models for Indoor Wireless Communications in Multifloored Buildings*, IEEE Transactions on Antennas and Propagation, Vol. 40, No. 2, 1992.

[23] Simon Lynen, Markus W. Achtelik, Stephan Weiss, Margarita Chli, Roland Siegwart, *A robust and modular multi-sensor fusion approach applied to MAV navigation*, IEEE/RSJ International Conference on Intelligent Robots and Systems (IROS), 2013

[24] Konstantinos Papakonstantinou, Dirk Slock, *ESPRIT-Based Estimation of Location and Motion Dependent Parameters*, Vehicular Technology Conference, 2009. VTC Spring 2009. IEEE 69th

[25] S. Al-Jazzar, J. Caffery *ESPRIT-based joint AOA/delay estimation for CDMA systems*, Wireless Communications and Networking Conference, 2004. WCNC. 2004 IEEE

[26] Helfenbein Tamás, Tóth András *Laser-Based Mobile Robot Positioning System*, ROBOTICS'08, VISION IN ROBOTICS. Brasov, 2008, pp. 323-330.

[27] Kun-Ming Yu, Ming-Gong Lee, Hung-Nien Hsieh, Wu-Cheng Lai *Implementation of an RFID-Based Virtual Signal Mechanism for an Indoor Location Sensing System*, Journal of Internet Technology, 02.2013

[28] Fraunhofer IIS *BLACKFIR Adaptive Localization Technologies*, https://www.iis.fraunhofer.de/en/ff/lv/lok.html Visited:2017.10.15

Tamás Helfenbein received the M.Sc. degree from the Budapest University of Technology and Economics (BME) in 2008. Between 2006 and 2008, he worked on the research and development of information and database systems of large datasets at the Research Institute of Physics (KFKI), Hungarian Academy of Sciences (HAS). From 2006, he is a lecturer of database and information systems courses at Forrai School. Between 2008 and 2011, during he was attended the doctoral school of BME, he worked as a scholar researcher at the Bay Zoltán Foundation for Applied Research (BZAKA). At the foundation and the university, he participated in several international research and development projects on machine vision, image processing, wireless sensor systems and ambient intelligence. From 2008, he teaches laboratory measurement practices at the university. From 2008-2014, he was working as a lead researcher at the Institute of Infocommunications Technology, Bay Zoltán Nonprofit Ltd. for Applied Research (BAY-IKTI), and currently, he is working as a researcher at Chebio Ltd. and focuses on embedded systems, wireless sensor networks, image processing, and machine vision as main research areas.

Roland Király In 2002 he graduated from Eszterházy Károly University as an ICT teacher. He gained his MSc in 2005 at Veszprém University. He attended his PhD course at the Institute of Informatics at ELTE University and obtained doctorate in 2015. He has been teaching at Eszterházy Károly University since 2002, now he is an associate professor of the Institute of Mathematics and Informatics. Between 2006 – 2012, he was a member of a research team dealing with Refactoring Erlang Programs at ELTE Univerity. In 2011, he was appointed the Secretary of the Magyar Rektori Tanács Informatikai és Tudományos Bizottság. Since 2013, he has been the head of the EKF RFID/NFC research team. This research focuses on the RFID/NFC technologies and Future Internet. In 2007, 2008 and 2009 – he received scolarship at Eötvös Lóránd University – Institute of Informatics IKKK. In 2013 and 2014, he received Jedlik Ányos Doctoral Scolarship for research activities. This research was supported by the European Union and the State of Hungary, co-financed by the European Social Fund in the framework of TÁMOP 4.2.4. A/2-11-1-2012-0001 National Excellence Program.

Márton Törőcsik has a Master's degree in Electrical Engineering, which he earned at Óbuda University. His thesis work was in Phase-locked Loop technique. Currently he works at Bay Zoltán Nonprofit Ltd. for Applied Research as a researcher, and works in the field of RFID and RF based localisation.

Emil Tóth received the M.Sc. degree as an electrical engineer from the Budapest University of Technology and Economics (BME) in 2013. During the M.Sc. studies his main research field was radar technology, especially Synthetic-aperture radar (SAR) and X band imaging. His thesis dealt with SAR imaging of the International Space Station. Since 2013 he works at the Bay Zoltán Nonprofit Ltd. for Applied Research as a researcher. He contributed with signal processing expertise in several projects related to the field of RF-based localization, the design and implementation of localization algorithms. Currently he works on developing mobile-based localization technologies.

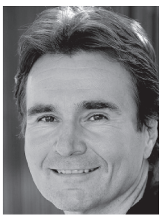

Sándor Király in 1995 he graduated from the University of Debrecen as an ICT teacher. He attended his PhD course at the Institute of Informatics at the University of Debrecen and obtained doctorate in 2013. He has been teaching at Eszterházy Károly College since 2010, now he is an associate professor of the Institute of Mathematics and Informatics. Since 2013, he has been working as a researcher in the EKF RFID/NFC research team. This research focuses on the RFID/NFC technologies and Future Internet.

Biennial since 1998

CSNDSP 2018

11th IEEE/IET International Symposium on Communication Systems, Networks and Digital Signal Processing

18–20 July 2018 | Budapest, Hungary
Danubius Health Spa Resort Margitsziget****

Invitation

Budapest welcomes the opportunity to host the 11th International Symposium on Communication Systems, Networks, and Digital Signal Processing.

The aim of CSNDSP 2018 is to serve as a forum for the exchange of ideas among engineers, scientists and young researchers from all over the world on advances in communication systems, communications networks and digital signal processing and to provide a focus for future research and developments.

Budapest is a city of water and spas, rendered magical by the Danube River connecting the nations and people of Europe. Hilly landscapes, long history, pleasant climate, rich cultural events, and music prove that the city is indeed a pearl of the Danube. An excellent venue in a peaceful environment and conference hotels are awaiting the guests. Budapest is one of the nicest cities in Europe, easy to reach, and famous for its hospitality, fine food, tasty drinks, and many historical and cultural sites of interest.

We wish you a pleasant and fruitful stay in Budapest during the conference.

The Hungarian Organising Committee

Main topics

- Communications Systems and Theory
- DSP
- Communications Protocols
- Networks & Network Management
- Photonics
- Wireless Networks
- Special Topic

The full list of our topics is available at the official website:

http://csndsp2018.com

Important dates

Full Paper (for review) due
12 February 2018

Notification of acceptance
starts 15 April 2018

Camera ready paper
ends 20 May 2018

Local Organising Committee

- **Eszter Udvary**
- **Zsolt Kollár**
- **Barna Csuka**
- **Lajos Nagy**
- **Gergely Mészáros**
- **Zoltán Szalay**

Steering Committee

- **Prof. Z. Ghassemlooy**
  Northumbria University, UK
  Chairman
- **Prof. Anthony C. Boucouvalas**
  University of Peloponnese, Tripoli, Greece
- **Prof. R. A. Carrasco**
  Newcastle University, UK
- **Prof. E. Leitgeb**
  Graz University of Technology, Austria
- **Prof. M. D. Logothetis**
  University of Patras, Greece
- **Dr. Wai Pang Ng**
  Northumbria University, UK
- **Prof. Stanislav Zvanovec**
  Czech Technical University in Prague, Czech Republic

Organised by:

MŰEGYETEM 1782

BME Faculty of Electrical Engineering and Informatics

Magyar Tudományos Akadémia 1825

For further information please visit
http://csndsp2018.com

Call for Papers

The ACM SIGCOMM 2018 conference seeks papers describing significant research contributions to the field of data communication networks and networked systems. SIGCOMM'18 takes a broad view of networking research. This includes new ideas relating to (but not limited to) mobile, wide-area, data-center, home, and enterprise networks using a variety of link technologies (wired, wireless, visual, and acoustic), as well as social networks and network architecture. It encompasses all aspects of networks and networked systems, including packet-processing hardware and software, virtualization, mobility, sensors, provisioning and resource management, performance, energy consumption, topology, robustness and security, measurement, diagnosis, verification, privacy, economics and evolution, interactions with applications, internet-of-things, novel applications of machine learning to networking, and usability of underlying networking technologies.

We want SIGCOMM'18 to be daring and emphasize novelty and creativity. The more novel the concept, the harder it can be to fully develop or evaluate all aspects, and the review process will take this into account. We encourage authors to discuss not only the benefits but also the limitations of their ideas.

Unlike in previous years, SIGCOMM'18 will not have a separate experience track. However, we do encourage the submission of experience papers that provide detailed technical insight into real-world deployments of novel networking technologies and systems.

In addition to the main conference, SIGCOMM 2018 will have a series of co-located workshops, tutorials, poster and demo sessions, a travel grant program, and conference best paper and SIGCOMM awards.

Submissions

SIGCOMM is a highly selective conference where papers report novel results typically substantiated by experimentation, deployment, simulation, or analysis. Submissions should be in two-column, 10-point format, and can be up to 12 pages in length with as many additional pages as necessary for references. Detailed submission instructions can be found on the conference web site.

Ethical Concerns

Authors must as part of the submission process attest that their work complies with all applicable ethical standards of their home institution(s), including, but not limited to privacy policies and policies on experiments involving humans. Note that submitting research for approval by one's institution's ethics review body is necessary, but not sufficient – in cases where the PC has concerns about the ethics of the work in a submission, the PC will have its own discussion of the ethics of that work. The PC takes a broad view of what constitutes an ethical concern, and authors agree to be available at any time during the review process to rapidly respond to queries from the PC chairs regarding ethical standards.

Important Dates

- Abstract submission: Wednesday, January 24, 2018
- Paper submission: Wednesday, January 31, 2018
- Reviews returned to authors: Friday May 11, 2018
- Technical program: August 20 - 24, 2018

Sponsors

Association for Computing Machinery

acm sigcomm

sigcomm Budapest 2018

The Wireless Days Conference is a major international conference which aims to bring together researchers, technologists and visionaries from academia, research centers and industry, engineers and students to exchange, discuss, and share their experiences, ideas and research results about theoretical and practical aspects of wireless networking. Wireless Days 2017 is technically co-sponsored by IEEE Communications Society and IFIP.

After the successful editions of 2008 in Dubai, UAE (44% acceptance ratio), 2009 in Paris, France (38% acceptance ratio), 2010 in Venice, Italy (33% acceptance ratio), 2011 in Niagara Falls, Canada (35% acceptance ratio), 2012 in Dublin, Ireland (35% acceptance ratio), 2013 in Valencia, Spain (34% acceptance ratio), 2014 Rio de Janeiro, Brazil, 2016 Toulouse, France (35% acceptance ratio), 2017 Porto, Portugal (XX% acceptance ratio), the tenth edition of Wireless Wireless Days will be held in Dubai, UAE, on April 3-5, 2018.

Wireless Days 2018 will include presentations of both theoretical and experimental achievements, innovative wireless systems, prototyping efforts, case studies and advances in technology related to wireless networking and communication infrastructures.

The Wireless Days 2018 program will be split into the following 5 conference tracks:

- **Track 1: 5G and Beyond**
- **Track 2: Wireless Communications**
- **Track 3: Ad Hoc, Sensor, Vehicular and Delay Tolerant Networks**
- **Track 4: Wireless Models and Simulations**
- **Track 5: Mobile Networking and Computing**

Paper Submission:

Authors should submit their papers online through the EDAS conference management system: http://edas.info/N23963

Submissions must be limited to 6 double-column pages (maximum of 2 additional pages allowed - 8 pages in total – with over-length page fee) and must follow the IEEE Manuscript template for conference proceedings: IEEE Manuscript template.

All submitted papers will be judged based on their originality, technical and/or research content, correctness, relevance to conference, contributions, and readability. Submitted papers will be peer-reviewed by the international technical program committee. Accepted and presented papers will be published in the conference proceedings.

All accepted and presented papers will be submitted for publication in IEEE Xplore Digital Library

Important Dates:

Paper Submission – November 7, 2017
Acceptance notification – January 15, 2018
Camera ready – February 15, 2018

Organizing Committee

General Chairs
- Adel Ben Mnaouer (Canadian University of Dubai, UAE)
- Mario Gerla (UCLA, USA)
- Catherine Rosenberg (University of Waterloo, Canada)

TPC Chair
- Nadjib Achir (University of Paris 13, France)
- Megumi Kaneko (National Institute of Informatics, Japan)

Keynotes Chair
- Raouf Boutaba (University of Waterloo, Canada)

Track 1 Chairs: 5G and Beyond
- Rolland Vida (Budapest University, Hungary)
- Michele Nogueira (UFPR, Brazil)
- Thierry Gayraud (LAAS, France)

Track 2 Chairs: Wireless Communications
- Luis Costa (Federal University of Rio de Janeiro, Brazil)
- Marc St-Hilaire (Carleton University, Canada)
- Yacine Ghamri Doudane (University of La Rochelle, France)

Track 3 Chairs: Ad Hoc, Sensor, Vehicular and Delay Tolerant Networks
- Manuel Ricardo (University of Porto, Portugal)
- Claudio Palazzi (University degli Studi di Padova, Italy)

Track 4 Chairs: Wireless Models and Simulations
- Carlos T. Calafate (Universitat Politecnica de Valencia, Spain)
- André-Luc Beylot (Université de Toulouse, France)
- Khaled Boussetta (University of Paris 13, France)

Track 5 Chairs: Mobile Networking and Computing
- Juan-Carlos Cano (Universitat Politecnica de Valencia, Spain)
- Nadjib Aitsaad (ESIEE Paris, France)
- Rui Campos (INESC TEC, Portugal)

Publicity Chairs:
- Miguel Elias Mitre Campista (UFRJ, Brazil)
- Soufiene Djahel (University College Dublin, Ireland)
- Abduhalim Dandoush (ESM, France)

Overall Arrangements
- Aziza Lounis (DNAC, France)

For more information visit:
http://www.wireless-days.com

Organized by DNAC, UPMC Sorbonne Universités, Université Paris 13

Supported by NII Inter-University Research Institute Corporation / Research Organization of Information and Systems National Institute of Informatics, La Rochelle Université, Canadian University of Dubai

Technical Sponsor IEEE, IEEE ComSoc IEEE Communications Society, ifip, ifip tc6

3rd Cloudifcation of the Internet of Things Conference

CIoT 2018

July 2 - 4, 2018
Paris, France

www.ciot-conference.org

The third edition of Cloudification of the Internet of Things 2018 (CIoT'18) is a conference focusing on the challenges of the Internets of Things while considering the whole end-to-end architecture based on 5G and Cloud solutions. In fact, the 5G network will absorb the billions of flows generated by things while considering the requested QoS and the cohabitation of M2M, M2H and H2M flows. Then, the flows will be processed in data centers and SaaS (applications) can exploit the generated knowledge.
The main objective of CIoT'18 is to address all the challenges of IoT systems from the sensors/machines to the end-users attached to the Cloud while considering the 5G network connecting both sides: IoT and Cloud domains. The conference covers all research and novel papers tackling but not limited to:

- **5G cellular networks (3GPP, ETSI, IEEE, etc.)**
- **Slicing solutions**
- **Cloud/ Fog solutions**
- **Software Defined Network (SDN) for IoT/5G/Cloud**
- **Network Function Virtualization (NFV) for IoT/5G/Cloud**
- **Architecture and protocols for IoT/5G/Cloud**
- **Green communication for IoT/5G/Cloud**
- **Centralized and distributed systems for IoT/5G/Cloud**
- **Management system for IoT/5G/Cloud**
- **Security for IoT/5G/Cloud**
- **Routing/MAC for IoT/5G/Cloud**
- **Big data for IoT/5G/Cloud**
- **Testbed and experimental platforms for IoT/5G/Cloud**
- **etc.**

Instructions for submission

The authors are invited to submit high-quality original technical papers for presentation at the conference and publication in the CIoT'18 Proceedings. All final submissions should be written in English. The paper length is 6 pages (10-point font). One or two additional pages can be accepted without any extra charges. Standard IEEE conference templates for LaTeX formats are found at here: http://www.ieee.org/conferences_events/conferences/publishing/templates.html
At least one author of each accepted presentation must register to the conference and present the paper. All papers must be submitted in electronic form through the EDAS web site at https://edas.info/N23586 by the deadline.

All the accepted papers will be published in IEEE Xplore.
The three best CIoT'18 papers will be invited to submit extended versions of their papers to Annals of Telecommunications with a fast review process. Annals of Telecommunications is published by Springer, and indexed in ISI and Scopus Databases.

The impact factor of Annals of Telecommunications in 2016 is 1.412
You will find additional information on our web site at:
www.ciot-conference.org

Keynote Speakers

Henning Schulzrinne (Columbia University, US)
Raouf Boutaba (University of Waterloo, Canada)
Thierry Coupaye (Orange Labs, France)

Important Dates

Paper submission deadline: February 2, 2018
Acceptance Notification: March 30, 2018
Camera Ready: April 13, 2018

General Chairs
- Blondia Chris (University of Antwerp, Belgium)
- Nadjib Aitsaadi (ESIEE Paris, France)
- Harry Perros (NCSU, USA)

TPC Co-Chairs
- Hassnaa Moustafa (Intel Labs, USA)
- Ilhem Fajjari (Orange Labs, France)

Keynotes Chair:
- Filip De Turck (Ghent University-imec, Belgium)

Tutorials Co-Chairs
- Mohamed Faten Zhani (École de technologie supérieure, Canada)
- Walter Cerroni (University of Bologna, Italy)

Demonstration Co-Chairs
- Marc-Oliver Pahl (TUM, Germany)
- Alberto Schaeffer-Filho (UFRGS, Brazil)

Steering Committee
- Guy Pujolle (UPMC, France)
- Raouf Boutaba (University of Waterloo, Canada)
- Harry Perros (NCSU, USA)
- Yutaka Takahashi (Kyoto University, Japan)
- Nadjib Aitsaadi (ESIEE Paris, France)
- Nathalie Mitton (INRIA, France)

Publicity Chairs
- Abdulhalim Dandoush (ESME Sudria, France)
- Yazid Lyazidi (UPMC, France)

Organization Committee Chair
- Aziza Lounis (DNAC, France)

Technical Sponsor

Sponsors

Organized by

Sponsorship requests are in progress

Guidelines for our Authors

Format of the manuscripts

Original manuscripts and final versions of papers should be submitted in IEEE format according to the formatting instructions available on
http://www.ieee.org/publications_standards/publications/authors/authors_journals.html#sect2,
"Template and Instructions on How to Create Your Paper".

Length of the manuscripts

The length of papers in the aforementioned format should be 6-8 journal pages.
Wherever appropriate, include 1-2 figures or tables per journal page.

Paper structure

Papers should follow the standard structure, consisting of *Introduction* (the part of paper numbered by "1"), and *Conclusion* (the last numbered part) and several *Sections* in between.
The Introduction should introduce the topic, tell why the subject of the paper is important, summarize the state of the art with references to existing works and underline the main innovative results of the paper. The Introduction should conclude with outlining the structure of the paper.

Accompanying parts

Papers should be accompanied by an *Abstract* and a few *index terms (Keywords)*. For the final version of accepted papers, please send the *short cvs* and *photos* of the authors as well.

Authors

In the title of the paper, authors are listed in the order given in the submitted manuscript. Their full affiliations and e-mail addresses will be given in a footnote on the first page as shown in the template. No degrees or other titles of the authors are given. Memberships of IEEE, HTE and other professional societies will be indicated so please supply this information. When submitting the manuscript, one of the authors should be indicated as corresponding author providing his/her postal address, fax number and telephone number for eventual correspondence and communication with the Editorial Board.

References

References should be listed at the end of the paper in the IEEE format, see below:

a) Last name of author or authors and first name or initials, or name of organization
b) Title of article in quotation marks
c) Title of periodical in full and set in italics
d) Volume, number, and, if available, part
e) First and last pages of article
f) Date of issue

[11] Boggs, S.A. and Fujimoto, N., "Techniques and instrumentation for measurement of transients in gas-insulated switchgear," IEEE Transactions on Electrical Installation, vol. ET-19, no. 2, pp.87–92, April 1984.

Format of a book reference:

[26] Peck, R.B., Hanson, W.E., and Thornburn, T.H., Foundation Engineering, 2nd ed. New York: McGraw-Hill, 1972, pp.230–292.

All references should be referred by the corresponding numbers in the text.

Figures

Figures should be black-and-white, clear, and drawn by the authors. Do not use figures or pictures downloaded from the Internet. Figures and pictures should be submitted also as separate files. Captions are obligatory. Within the text, references should be made by figure numbers, e.g. "see Fig. 2."
When using figures from other printed materials, exact references and note on copyright should be included. Obtaining the copyright is the responsibility of authors.

Contact address

Authors are requested to submit their papers electronically via the EasyChair system. The link for submission can be found on the journal's website:
www.infocommunications.hu/for-our-authors

If you have any question about the journal or the submission process, please do not hesitate to contact us via e-mail:

Rolland Vida – Editor-in-Chief:
vida@tmit.bme.hu

Árpád Huszák – Associate Editor-in-Chief:
huszak@hit.bme.hu

SCIENTIFIC ASSOCIATION FOR INFOCOMMUNICATIONS

SCIENTIFIC ASSOCIATION FOR INFOCOMMUNICATIONS HUNGARY

FOUNDED IN 1949

Who we are

Founded in 1949, the Scientific Association for Infocommunications (formerly known as Scientific Society for Telecommunications) is a voluntary and autonomous professional society of engineers and economists, researchers and businessmen, managers and educational, regulatory and other professionals working in the fields of telecommunications, broadcasting, electronics, information and media technologies in Hungary.

Besides its 1000 individual members, the Scientific Association for Infocommunications (in Hungarian: HÍRKÖZLÉSI ÉS INFORMATIKAI TUDOMÁNYOS EGYESÜLET, HTE) has more than 60 corporate members as well. Among them there are large companies and small-and-medium enterprises with industrial, trade, service-providing, research and development activities, as well as educational institutions and research centers.

HTE is a Sister Society of the Institute of Electrical and Electronics Engineers, Inc. (IEEE) and the IEEE Communications Society.

What we do

HTE has a broad range of activities that aim to promote the convergence of information and communication technologies and the deployment of synergic applications and services, to broaden the knowledge and skills of our members, to facilitate the exchange of ideas and experiences, as well as to integrate and harmonize the professional opinions and standpoints derived from various group interests and market dynamics.

To achieve these goals, we…

- contribute to the analysis of technical, economic, and social questions related to our field of competence, and forward the synthesized opinion of our experts to scientific, legislative, industrial and educational organizations and institutions;
- follow the national and international trends and results related to our field of competence, foster the professional and business relations between foreign and Hungarian companies and institutes;
- organize an extensive range of lectures, seminars, debates, conferences, exhibitions, company presentations, and club events in order to transfer and deploy scientific, technical and economic knowledge and skills;
- promote professional secondary and higher education and take active part in the development of professional education, teaching and training;
- establish and maintain relations with other domestic and foreign fellow associations, IEEE sister societies;
- award prizes for outstanding scientific, educational, managerial, commercial and/or societal activities and achievements in the fields of infocommunication.

Contact information

President: **GÁBOR MAGYAR, PhD** • *elnok@hte.hu*

Secretary-General: **ERZSÉBET BÁNKUTI** • *bankutie@ahrt.hu*

Operations Director: **PÉTER NAGY** • *nagy.peter@hte.hu*

International Affairs: **ROLLAND VIDA, PhD** • *vida@tmit.bme.hu*

Address: H-1051 Budapest, Bajcsy-Zsilinszky str. 12, HUNGARY, Room: 502

Phone: +36 1 353 1027

E-mail: *info@hte.hu*, Web: *www.hte.hu*